

Schwendel, Arved ORCID logoORCID:

<https://orcid.org/0000-0003-2937-1748>, Nicholas, Andrew P., Aalto, Rolf E., Sambrook Smith, Greg H. and Buckley, Simon (2015) Interaction between meander dynamics and floodplain heterogeneity in a large tropical sand-bed river: the Rio Beni, Bolivian Amazon. *Earth Surface Processes and Landforms*, 40 (15). pp. 2026-2040.

Downloaded from: <https://ray.yorks.ac.uk/id/eprint/2620/>

The version presented here may differ from the published version or version of record. If you intend to cite from the work you are advised to consult the publisher's version:

<https://doi.org/10.1002/esp.3777>

Research at York St John (RaY) is an institutional repository. It supports the principles of open access by making the research outputs of the University available in digital form. Copyright of the items stored in RaY reside with the authors and/or other copyright owners. Users may access full text items free of charge, and may download a copy for private study or non-commercial research. For further reuse terms, see licence terms governing individual outputs. [Institutional Repository Policy Statement](#)

RaY

Research at the University of York St John

For more information please contact RaY at ray@yorks.ac.uk

**Earth Surface
Processes and Landforms**

**Interaction between meander dynamics and floodplain
heterogeneity in a large tropical sand-bed river: the Rio
Beni, Bolivian Amazon**

Journal:	<i>Earth Surface Processes and Landforms</i>
Manuscript ID:	ESP-14-0250.R3
Wiley - Manuscript type:	Paper
Date Submitted by the Author:	n/a
Complete List of Authors:	Schwendel, Arved; University of Exeter, College of Life and Environmental Sciences Nicholas, Andrew; University of Exeter, College of Life and Environmental Sciences Aalto, Rolf; University of Exeter, College of Life and Environmental Sciences Sambrook Smith, Greg; University of Birmingham, School of Geography, Earth & Environmental Sciences Buckley, Simon; University of Exeter, College of Life and Environmental Sciences
Keywords:	Meander migration, floodplain heterogeneity, bank erosion, numerical model, planform evolution

SCHOLARONE™
Manuscripts

Interaction between meander dynamics and floodplain heterogeneity in a large tropical sand-bed river: the Rio Beni, Bolivian Amazon

Schwendel A.C.¹, Nicholas A.P.¹, Aalto R.E.¹, Sambrook Smith G.H.², Buckley S.¹

¹ College of Life and Environmental Sciences - Geography, University of Exeter, Exeter, EX4 4RJ UK

² School of Geography, Earth & Environmental Sciences , University of Birmingham, Birmingham , B15 2TT, UK

Abstract

The evolution of meandering river floodplains is predominantly controlled by the interplay between overbank sedimentation and channel migration. The resulting spatial heterogeneity in floodplain deposits leads to variability in bank erodibility, which in turn influences channel migration and planform development. Despite the potential significance of these feedbacks, few studies have quantified their impact upon channel evolution and floodplain construction in dynamic settings (e.g., locations characterized by rapid channel migration and high rates of overbank sedimentation). This study employs a combination of field observations, GIS analysis of satellite imagery and numerical modelling to investigate these issues along a 375 km reach of the Rio Beni in the Bolivian Amazon. Results demonstrate that the occurrence of clay-rich floodplain deposits promotes a significant reduction in channel migration rates and distinctive styles of channel evolution, including channel straightening and immobilisation of bend apices leading to channel narrowing. Clay bodies act as stable locations limiting the propagation of planform disturbances in

both upstream and downstream directions, and operate as 'hinge' points, around which the channel migrates. Spatial variations in the erodibility of clay-rich floodplain material also promote large-scale (10-50 km) differences in channel sinuosity and migration, although these variables are also likely to be influenced by channel gradient and tectonic effects that are difficult to quantify. Numerical model results suggest that spatial heterogeneity in bank erodibility, driven by variable bank composition, may force a substantial (c. 30%) reduction in average channel sinuosity, compared to situations in which bank strength is spatially homogeneous.

32

33 **Keywords**

34 Meander migration; floodplain heterogeneity; bank erosion; numerical model;
35 planform evolution

1
2
3
4
5
6
7
8
9
10
11
12
13
14
15
16
17
18
19
20
21
22
23
24
25
26
27
28
29
30
31
32
33
34
35
36
37
38
39
40
41
42
43
44
45
46
47
48
49
50
51
52
53
54
55
56
57
58
59
60

36 **Introduction**

37 Understanding the relationship between meander migration and floodplain evolution
38 is important for a wide range of issues, including river bank erosion and widening,
39 supply of bedload and suspended sediment to the channel, and the associated
40 deposition of sediment on in-channel bars and floodplain surfaces (Nanson and
41 Hickin, 1986; Salo et al., 1986; Lauer and Parker, 2008). Moreover, these processes
42 represent key controls on channel conveyance capacity, flood frequency, long-term
43 floodplain morphodynamics and the ecological functioning of the channel-floodplain
44 environment (Ward et al., 2002; Gueneralp et al., 2012). These issues are thus a
45 primary concern in many areas of river management, including river restoration,
46 floodplain land use and contamination, flood prevention and navigation.

47 The dynamics of meandering rivers has been the subject of intense research
48 over the past four decades, from multiple perspectives. For example, many studies
49 have attempted to classify channel behaviour (e.g., Brice, 1974; Hickin, 1974;
50 Hooke, 1984; Hooke, 2003) and reproduce or explain it using mathematical models
51 (e.g., Ikeda et al., 1981; Ferguson, 1984; Howard and Knutson, 1984; Johannesson
52 and Parker, 1989; Howard, 1992; Zolezzi and Seminara, 2001). Migration of bends
53 has often been explored with respect to freely-meandering rivers in relatively
54 homogeneous floodplains, where characteristic planform patterns have been
55 described (e.g., Hooke, 1995). Numerical models have been shown to be capable of
56 generating realistic planform configurations (Lancaster and Bras, 2002; Camporeale
57 et al., 2005; Frascati and Lanzoni, 2010), including compounding bends, asymmetric
58 up-valley skewing and formation of multi-bend loops. However, understanding of the
59 role of variability in bank strength as a control on meander migration remains
60 incomplete.

Variable resistance to erosion of river banks may be due to vegetation (Perucca et al., 2007), slump blocks (Parker et al., 2011), drift wood, sedimentology and pedological evolution of bank sediments (Constantine et al., 2009), bedrock (Limaye and Lamb, 2014) or differences in bank height (van de Wiel and Darby, 2007; Xu et al., 2011). Numerous studies have investigated how such variations in bank strength impact on meander migration (e.g., Howard, 1996; Sun et al., 1996; Huang and Nanson, 1998; Hudson and Kesel, 2000; Seminara, 2006, Gueneralp and Rhoads, 2011; Motta et al., 2012a; Posner and Duan, 2012; Limaye and Lamb, 2014). However, the majority of this work has been based on numerical modelling rather than empirical evidence, due to the relatively short record of high quality imagery (e.g. c. 40 years in the case of satellite data) available for the study of channel migration at high temporal resolutions. Modelling studies suggest that a decrease in channel belt width may occur where bank erodibility is spatially heterogeneous (Sun et al., 1996; Gueneralp and Rhoads, 2011). However, the implications for meander geometry remain to be resolved fully. For example, Sun et al. (1996) found that floodplain heterogeneity has a limited impact on bend wavelength, while Gueneralp and Rhoads (2011) show that it may promote compound bends and downstream-skewing of meanders normally associated with super-resonant conditions (Camporeale and Ridolfi, 2006; Seminara, 2006). Huang and Nanson (1998) found an influence of variable bank strength on channel geometry, in particular width, but indicate that its impact is limited compared to hydraulic factors.

Significantly, several modelling studies have examined the effects of a random spatial distribution of floodplain erodibility (e.g., Gueneralp and Rhoads, 2011) or have employed a stochastic model in which mean erodibility decreases with

1
2
3
4
5
6
7
8
9
10
11
12
13
14
15
16
17
18
19
20
21
22
23
24
25
26
27
28
29
30
31
32
33
34
35
36
37
38
39
40
41
42
43
44
45
46
47
48
49
50
51
52
53
54
55
56
57
58
59
60

86 distance from the channel (e.g., Motta et al., 2012a). These studies demonstrate the
87 scale-dependent influence of floodplain heterogeneity on channel planform
88 complexity. However, floodplain heterogeneity is unlikely to vary in a way that is
89 random, but is instead likely to be controlled by the spatial scaling of, and
90 interactions between, floodplain morphology, hydrodynamics, vegetation, and
91 sedimentation processes. Thus the role of sedimentary heterogeneity in floodplain
92 evolution and meander migration requires further research (Güneralp et al., 2012),
93 particularly in the context of the complexity found in natural landscapes.

94 The aim of this paper is to quantify the influence of variations in bank
95 composition on meander migration within large, dynamic sand-bed rivers, using field
96 and remote sensing datasets obtained from the Rio Beni in the Bolivian Amazon.
97 The specific objectives of the work are threefold: First, to assess the influence of
98 bank material on rate and style of channel migration at individual meander bends.
99 Second, to examine channel evolution over multiple bends, in order to elucidate the
100 role of floodplain heterogeneity as a control on large-scale channel belt
101 characteristics and on the propagation of planform irregularities between bends.
102 Third, to explore the potential for simulating and explaining these characteristics
103 using a simple numerical model of meander migration.

104

105 **Study site**

106 The Rio Beni was chosen for this study due to its extensive floodplain, which is
107 essentially undisturbed by human influence, and its high rates of meander migration
108 and floodplain sedimentation within a single active channel belt. The reach of the Rio
109 Beni examined herein is located in the Andean foreland basin in north-eastern

1
2
3 110 Bolivia (Fig. 1), and has been largely unaffected by the effects of Holocene sea level
4
5 111 change. The upstream end of this reach is near Rurrenabaque, where the Beni
6
7 112 leaves the piedmont of the Andes (Serrania el Susi) and meanders for approximately
8
9 113 375 km (channel length) through the forested 'Llanos de Mojos', a floodplain built up
10
11 114 of late-Miocene and Quaternary sediments (Dumont, 1996; Gautier et al., 2007).
12
13 115 Catchment area at Rurrenabaque is 68,000 km² (Gautier et al., 2010), mean channel
14
15 116 width at low flow is 430 m, mean discharge is 2,300 m³s⁻¹, and annual flood peaks
16
17 117 frequently exceed 20,000 m³s⁻¹ (Environmental Research Observatory (ORE)
18
19 118 HyBAm). The Rio Beni transports a comparatively high sediment load of 219 x 10⁶ t
20
21 119 a⁻¹ (Latrubesse and Restrepo, 2014), which can be characterised as of fresh Andean
22
23 120 origin (Guyot et al., 2007) and constitutes 72% of the load of the Rio Madeira (Guyot
24
25 121 et al., 1999).
26
27
28
29

30 122 Water surface slope decreases dramatically within the upstream section of the
31
32 123 study reach where the Rio Beni leaves the piedmont fan and bed material changes
33
34 124 from cobble-gravel to sand. Downstream of this point, channel slope declines from
35
36 125 0.0002 to 0.00007 m m⁻¹ over a distance of 300 km. Beyond this (over the final 75
37
38 126 km) the river profile steepens, although the paucity of reliable dGPS data make it
39
40 127 difficult to quantify the gradient with confidence (see also Gautier et al., 2007). Mean
41
42 128 channel sinuosity within the study reach varies temporally (between 1.8 and 2.0) and
43
44 129 spatially amongst sub-reaches (between 1.3 and 2.7) (see also Dumont, 1996,
45
46 130 Gautier et al., 2007). Downstream of the piedmont fan, median sediment size of bed
47
48 131 and suspended load is relatively constant ranging between 0.09 - 0.15 mm and
49
50 132 0.0094 - 0.012 mm respectively (Guyot et al., 1999). The channel and its proximal
51
52 133 floodplain are largely unaffected by anthropogenic modification such as bank
53
54 134 protection, dredging or deforestation (Aalto et al., 2003).
55
56
57
58
59
60

1
2
3
4
5
6
7
8
9
10
11
12
13
14
15
16
17
18
19
20
21
22
23
24
25
26
27
28
29
30
31
32
33
34
35
36
37
38
39
40
41
42
43
44
45
46
47
48
49
50
51
52
53
54
55
56
57
58
59
60

135 The Beni channel belt has experienced a counterclockwise shift from a
136 northeast orientation (a position currently occupied by the Rio Yacumu) to a more
137 northerly course during the Holocene (Plafker, 1964). Moreover, the deflection point
138 migrated northward following a north-striking fault line that separates old upper fluvial
139 terraces and hardened clay sediments in the NW from younger floodplain sediments
140 in the southeast (Dumont and Hannagarth, 1993; Dumont, 1996). The migration of
141 the channel belt also responds to differential subsidence and uplift patterns aligned
142 with southwest – northeast striking lineaments in the Brazilian Craton (Plafker, 1964;
143 Allenby, 1988).

144

145 **Methods**

146 Field data were acquired during visits to the study area between 2011 and 2013.
147 Data include measurements of water surface slope and ground elevation obtained
148 using dGPS (XRT, Trimble Navigation Ltd, Sunnyvale, USA) in conjunction with real-
149 time OmniSTAR HP correction or post-processing (CSRS-PrecisePointPositioning,
150 Natural Resources Canada, Ottawa, Canada). Relative bank height (the difference
151 between the bank top and low flow water level) was measured from a boat with a
152 dGPS supported laser range finder (Impulse 200 LR, Laser Technology Inc.,
153 Centennial, USA). These measurements were taken on cut bank and point bar sides
154 of bends and along straight sections in intervals of approximately 100 m. Differences
155 in bank composition were mapped using digital photographs of bank sections along
156 approximately 350 km of channel combined with sampling of bank sediments (n =
157 67) for laboratory grain size analysis, carried out using a Sedigraph 5100
158 (Micromeretics Instrument Corp., Norcross, USA). Bank material was sampled at a

159 number of heights above the water level at representative locations for each bank
160 material class.

161 Rates and styles of river migration were quantified by digitizing channel bank
162 lines in ArcGIS (ESRI, Redlands, USA) from geo-referenced multispectral Landsat
163 imagery (Table 1), taken during dry season (May to September), for 18 years
164 between 1975 and 2011 (Gautier et al., 2007). Additional bank lines were acquired
165 from aerial photography collected in 1960 (provided by the Bolivian Navy, see also
166 Plafker, 1964) that covered the upper 280 km of the study reach (Table 1). Individual
167 bends were numbered from the upstream end of the reach (117 bends in total). It
168 should be noted that not all bends are present over the entire period of study (due to
169 periodic bend initiation and abandonment). The study reach was divided into 19 sub-
170 reaches (mean length ~ 20 km) at locations where the channel has experienced only
171 minor lateral migration over the past 50 years (see Fig. 1).

172 Bank lines were converted to centrelines, which were then resampled to a
173 node spacing of 100 m (approximately a quarter of one mean channel width) for use
174 in subsequent analysis. Curvature was calculated following Motta et al. (2012b;
175 equation 15), while migration rate at bends was measured as the area between two
176 centrelines divided by the bend length, whereby bends are bounded in up- and
177 downstream directions by points of inflection of the centreline. Apparent migration
178 associated with centerline movement following bend cutoff has been excluded from
179 all calculations. It should be noted that migration rates calculated from image pairs
180 may be sensitive to the time period between images. For example, where the
181 channel does not move in a consistent direction over time the migration rate from a
182 single pair of images may be under-estimated (i.e. where the migration direction
183 reverses during the period covered by the image pair). Between 2003 and 2011,

1
2
3
4
5
6
7
8
9
10
11
12
13
14
15
16
17
18
19
20
21
22
23
24
25
26
27
28
29
30
31
32
33
34
35
36
37
38
39
40
41
42
43
44
45
46
47
48
49
50
51
52
53
54
55
56
57
58
59
60

184 errors introduced by image rectification were found to be negligible, due to precise
185 pre-rectification of the Landsat images. For older images, migration distances of less
186 than 16 m can be affected by image rectification errors ($RMSE < 16$ m relative to
187 2000 image; Table 1). The mean random error induced by pixel resolution (30 m) is
188 expected to be close to zero over an entire bank line.

189 Bend evolution was investigated at 117 bends over a period of 51 years. This
190 involved visual assessment of individual bends in ArcGIS and classification
191 according to channel migration style (see Fig. 2; see also Hooke, 1984). Styles of
192 migration include: a) longitudinal expansion or contraction of the bend (i.e., changes
193 in bend wave length); b) lateral extension or contraction (i.e., changes in bend
194 amplitude); c) confined or unconfined translation longitudinally up or down the valley;
195 d) lateral displacement (bend migration without alteration of planform shape between
196 points of inflection); e) bend rotation; and f) no change (stable). Complex, irregular
197 and compounding patterns were separated from simple bend evolution styles. Some
198 bends are characterised by mixed styles of migration involving several elements of
199 the behaviour outlined above. Thus this classification results in numerous
200 combinations of the basic types of channel change, which were then generalised and
201 grouped into 7 common migration styles in order to remove some of the subjectivity
202 introduced by the visual assessment. The focus of this classification is on dominant
203 style of migration and not the quantification of the magnitude of displacement.

204 In order to explore the relationship between channel geometry, migration rate
205 and bank erodibility further, numerical simulations were carried out using a simple
206 model of meander migration and floodplain sedimentation. The approach adopted
207 herein follows that of Howard (1992), differing only in the detail of the model
208 formulation (see below). Specifically, we simulate overbank sedimentation using a

form of exponential decay law, as is common in models of long-term floodplain evolution (e.g., Howard, 1992; Mackey and Bridge, 1995):

$$D_i = C_i H^{1.5} e^{-\alpha_i x} \quad (1)$$

where D_i is the deposition rate for size fraction i , C_i and α_i are a grain size dependent constant and decay coefficient, H is the height difference between the floodplain surface and an assumed maximum flood water level, and x is distance to the nearest channel. The non-linear dependence of D upon H reflects the increased frequency of inundation of low-lying floodplain areas. In the current model application, two grain size fractions have been used (one fine fraction and one coarse fraction). They are not intended to represent specific sediment sizes because the model should be considered phenomenological rather than physically-based. The parameters C_i and α_i were assigned values of 0.035 and 0.0015, respectively, for the coarse size fraction, and 0.005 and 0.00015, respectively, for the fine size fraction. These values were selected to approximate the decline in sedimentation rates and deposit grain size observed for the Beni by Aalto *et al.* (2003). This equation is applied over a grid of cells to update the floodplain grain size composition (and topography) during each model iteration.

Meander migration is simulated herein using the model of Howard and Knutson (1984), implemented using the parameterization that is equivalent to the approach of Ikeda *et al.* (1981). In this model, migration rates are a product of the weighted sum of local and upstream channel curvatures, and a local bank erodibility coefficient. Thus the detail of flow and sediment transport are not represented and channel migration is a function of planform geometry and bank strength only. Channel curvature is calculated from the coordinates of nodes spaced at one half

1
2
3
4
5
6
7
8
9
10
11
12
13
14
15
16
17
18
19
20
21
22
23
24
25
26
27
28
29
30
31
32
33
34
35
36
37
38
39
40
41
42
43
44
45
46
47
48
49
50
51
52
53
54
55
56
57
58
59
60

233 mean channel width along the centerline. Migration leads to movement of these
234 nodes and, ultimately, to neck cutoff (when two sections of channel migrate close to
235 one another). Chute cutoffs are not modelled herein, and are rare along the Beni.
236 Erodibility is defined as a function of the floodplain grain size composition in the grid
237 cell into which the channel is migrating. The relationship between bank erodibility (E)
238 and the fraction of the floodplain composed of fines (F) is represented by:

239
$$E = \beta(0.05+0.95(1-F)^k) \tag{2}$$

240 where β and k are constants. The value of β controls the average rate of channel
241 migration, but not the dependence of migration on floodplain heterogeneity. The
242 value of k determines the strength of the relationship between erodibility and bank
243 composition (a higher value of k yields a stronger grain size dependence). The form
244 of equation (2) was chosen by combining relationships between bank silt-clay
245 content, critical shear stress, and bank erosion rate presented by Julian and Torres
246 (2006; their Figures 4 and 6). They report an inverse relationship between critical
247 shear stress and bank erosion rates, which would lead to infinite erosion rates where
248 F tends to 0. Consequently, equation (2) is adopted herein, which overcomes this
249 problem and provides a good fit to the relationships shown by Julian and Torres
250 (2006) where $k = 6$. The combined bank erosion and floodplain sedimentation model
251 was implemented herein using $\beta = 4$ and $k = 6$, $\beta = 2$ and $k = 3$ (i.e. reduced
252 dependence of E on F), and $\beta = 1$ and $k = 0$ (i.e. bank erodibility independent of
253 floodplain grain size composition). Simulations used a floodplain domain with
254 dimensions of 125 km (downstream) by 50 km (cross-stream) and a grid resolution
255 of 500 m. The model is initialized using a flat floodplain and straight channel with
256 very small random perturbations in channel centerline coordinates.

Results

Rates and styles of migration at individual bends

Cutbanks characterised by clay-rich sediments (hereafter also termed clay banks) were mapped at 19 bends during several field visits between 2003 and 2011. Such banks were identified by their grain size assemblage and their distinctive colour and geometry. For example, clay-rich banks often contain ferrous concretions, giving them a speckled appearance, while on the lower bank the matrix material is often of a greyish colour, indicating oxygen depletion over prolonged periods (see Fig. 3). The coherent nature of these banks leads to a stable, often slightly less than vertical upper bank geometry, below which banks can have a scalloped shape with regular protrusions into the channel. The average grain size composition of banks identified visually as clay-rich was found to be 39-84% clay and 15-61% silt, compared with 15-25% clay and 75-83% silt in other bank sections. Sand constitutes a small fraction in most banks with a range of 0-11%. The D_{50} of bank material classified as clay-rich ranges between <0.6 and $3.42 \mu\text{m}$ but is typically smaller than $2 \mu\text{m}$. Although clay banks are unusually high in some places (e.g., due to tectonic uplift at the upstream end of the study site, in sub-reach 1) their mean height above low flow water level over the entire study reach (6.47 m) is not significantly higher than for banks composed of any other substrate (6.40 m) (two-sample t test, $\alpha = 0.05$). Moreover, there is no significant relationship between migration rate and bank height evident within the study reach as a whole (Pearson's $r = -0.24$, $p = 0.067$, $n = 61$).

Individual clay-rich banks vary in grain size, extent of reddish concretions, height and erodibility, which may reflect differences in their age and post-depositional development. Despite this variability, locations occupied by clay banks

1
2
3
4
5
6
7
8
9
10
11
12
13
14
15
16
17
18
19
20
21
22
23
24
25
26
27
28
29
30
31
32
33
34
35
36
37
38
39
40
41
42
43
44
45
46
47
48
49
50
51
52
53
54
55
56
57
58
59
60

281 experience significantly lower mean rates of channel migration at the scale of whole
282 bends (two-sample t test, $p < 0.05$) compared to bends with cutbanks made of any
283 other alluvial deposit (Fig. 4). Mean annual bend migration rate of individual bends
284 ranges between 3.4 ma^{-1} and 530.7 ma^{-1} . It is lowest at bends with clay banks (23.8
285 ma^{-1}), followed by bends migrating into mixed substrates (37.3 ma^{-1}), point bar
286 deposits (43.3 ma^{-1}) and infilled channels (58.8 ma^{-1}). Mean migration rate is highest
287 at bends migrating into oxbow lakes (98.8 ma^{-1}), although migration rates are highly
288 variable in such cases and depend on cutoff age (degree of fill), substrate
289 (erodibility) and angle of approach by the migrating bend. Mean annual bend
290 migration rates show a significant correlation ($\alpha = 0.05$) with a number of discharge
291 metrics such as accumulated discharge during wet seasons (December to April),
292 maximum annual discharge and the number of days with discharge in excess of
293 bankfull ($6000 \text{ m}^3 \text{ s}^{-1}$) with Pearson's r of 0.66, 0.71 and 0.82, respectively.
294 Correlations based on metrics that summarise the previous three wet seasons are
295 stronger than those based on the previous wet season only.

296 The channel in the region of clay banks is characterised by distinct narrowing
297 just downstream of the apex, often due to a resistant notch of clay protruding into the
298 channel (average channel width of 290 m in 2011, for $n = 22$ bends). Channel width
299 at the equivalent position for bends without clay banks is 534 m ($n = 63$). Despite the
300 particular planform configuration at these bends, no specific pattern in water surface
301 slope could be established. Bend migration rate is not correlated to mean slope at
302 various distances upstream of, downstream of, or around bend apices.

303 Classification of bend migration style (over the period from 1960 to 2011)
304 indicates that 28.1% of the bends are relatively immobile, as indicated by their low
305 mean rate of migration (26.0 ma^{-1}). Sub-reaches dominated by clay-rich banks

(especially sub-reaches 1 and 12, Fig. 5) are characterised by a high proportion of immobile bends. Wavelength expansion is apparent at 13.3% of bends, often in combination with bend rotation and/or changes in amplitude. This occurs mainly in the more mobile sub-reaches located in the central part of the study reach. In contrast 16.8% of bends experienced a reduction in wavelength, often accompanied by lateral extension (e.g., a common style in the early phase of bend development, just after bend inception) and/or rotation, but, in a few cases, also by a reduction in bend amplitude.

Channel belt widening, as signified by the bend extension and lateral displacement without a change in bend shape, occurs at 30.1% of bends, and is typical of mobile sub-reaches with few clay-rich banks (e.g., sub-reaches 6, 9, 10, 13, 16). Bend rotation is also prominent in these sub-reaches (11.1% of bends) and takes place more frequently in a downstream direction. Translation is experienced by 14.8% of bends, is most significant in sub-reaches 2, 4, 8 and 14, and is not preferentially associated with particular bank composition. Up-valley bend translation is rare and occurs mainly at a slow rate and is often associated with migration along a clay-rich bank. A small proportion (2.1%) of all bends showed signs of compounding and increased complexity. Compound bend development occurs in slowly expanding meanders (e.g., in sub-reach 17), as a result of flow diversion at bifurcations (e.g., in sub-reach 4) or partial contact with a clay body (e.g., in sub-reach 8).

Bends with clay-rich banks may share common planform and evolutionary characteristics, depending on the precise location of clay bodies. For example, migration of the apex of a bend into a clay body can lead to wavelength expansion, eventually followed by compounding (Fig. 2a). In the upstream part of the study reach the active channel belt appears to be confined by elongated clay bodies

1
2
3
4
5
6
7
8
9
10
11
12
13
14
15
16
17
18
19
20
21
22
23
24
25
26
27
28
29
30
31
32
33
34
35
36
37
38
39
40
41
42
43
44
45
46
47
48
49
50
51
52
53
54
55
56
57
58
59
60

331 parallel to the valley axis. In this region, the entire active cutbank of some bends
332 consists of clay-rich deposits, which usually render the bend immobile with limited
333 up- or down-valley translation (e.g., bend 13 up-valley, Fig. 6). In such cases, some
334 upstream rotation of the bend around the apex may occur. The downstream limb of
335 bends with clay-rich banks tends to elongate and straighten with time. Since
336 meanders not constricted by clay-rich banks typically have shorter life spans (i.e.
337 they evolve to cutoff more quickly), and higher rates of migration and down-valley
338 translation, bends located upstream of less mobile clay-rich meanders can appear to
339 move down-valley past the relative fixed apices of clay banks. As a result, bends
340 with clay-rich banks often appear in planform to be skewed up-valley, with the
341 downstream limb being laterally immobilised by contact with the clay-rich bank (e.g.,
342 bend 14 in Fig. 6). Consequently, over time, bends with clay-rich banks can
343 experience a reduction in wave length due to faster migration of the more mobile
344 upstream limb than of the downstream limb, which eventually leads to a neck cutoff.

345

346 **Planform evolution at multi-bend scales**

347 Downstream of clay banks the channel planform often exhibits straightening unless
348 influenced by contact with other clay bodies (Fig. 7). This process involves a gradual
349 reduction in sinuosity over several years, in contrast to rapid channel shortening due
350 to bend cutoff. Channel straightening usually involves an increase in wavelength and
351 contraction in amplitude of bends, for example confined downstream translation,
352 when the downstream limb of a bend translates faster down-valley than the
353 upstream limb (as visible in sub-reaches 1, 8, 10, 12). Such straightening
354 downstream of bends with clay-rich banks may be terminated when the bend in

question is cutoff. The steady lengthening of straight reaches can be accelerated by cutoffs, or slowed down or reversed where the channel that is straightening migrates into another clay body (dashed lines in Fig. 7), which introduces new bends and thus increases sinuosity. Moreover, in locations characterised by many closely spaced clay bodies, straights may be unable to form, and cutoffs may be frequent (e.g. sub-reaches 4 and 6). Sustained channel straightening over distances greater than 10 km and periods longer than 10 years is rare and only found in sub-reaches 7 and 15 in the last 50 years. For example, in the latter sub-reach, sinuosity declined from 1.31 to 1.24 over a 15 year period follow a cutoff in 1960. This process appears to have been induced by contact with the clay body on the western edge of the channel belt. More recently, the channel in sub-reach 7 (see Fig. 8) was characterised by straightening between 1998 and 2005 with a reduction in sinuosity from 1.82 to 1.32. Although this involved several cutoffs, these events were not followed by a gradual increase in sinuosity, which is a typical response to channel shortening (Hooke, 2003). In this case, straightening may have been initiated by contact between the channel and a clay body in bend 35 at the upstream end of the sub-reach (Fig. 8 a, b) as early as 1987. This triggered a series of neck cutoffs at bends 36 and 39 (Fig. 8 b and 8 c), accelerated bend migration down-valley, rapid planform adjustment via chute cutoffs at bends 41 and 43 (Fig. 8 d) and thus significant lengthening of the straight reach below bend 35 until 2005 (Fig. 8 e; see also Fig. 7). Although new planform perturbations developed upstream of former bend 39, the downstream translation of these perturbations has been impeded by a clay-rich bank at bend 40, which acts as a hinge with a fixed apex, thus limiting channel adjustment downstream (Fig. 8 e and 8 f). Consequently, the newly formed bend 38 has increased in amplitude and become gradually more asymmetric due to stabilisation of

1
2
3
4
5
6
7
8
9
10
11
12
13
14
15
16
17
18
19
20
21
22
23
24
25
26
27
28
29
30
31
32
33
34
35
36
37
38
39
40
41
42
43
44
45
46
47
48
49
50
51
52
53
54
55
56
57
58
59
60

380 the apex of bend 40, leading to a steady increase in sinuosity since 2005. The
381 overall tendency for clay-rich banks to induce channel straightening leads to an
382 abundance of channel sections with low planform curvature. Moreover, the
383 frequency distribution of channel curvature for sub-reaches with numerous clay bank
384 sections exhibits a distinct exponential form, compared to a more linear distribution
385 in other sub-reaches (Fig. 9).

386 The previous sections have highlighted the influence of clay banks on channel
387 form at the scale of individual bends and sub-reaches (lengths of c. 20 km). Spatial
388 variations in the frequency of clay bodies along the 375 km study reach also appear
389 to promote changes in channel dynamics at larger spatial scales, both in terms of
390 rates of bend migration and cutoff (Fig. 10) and channel sinuosity (Fig. 11). For
391 example, in the upper part of the study reach (sub-reaches 1 to 5 and the upstream
392 part of sub-reach 6) the active channel belt is laterally confined by clay bodies
393 (elements of the Chore and Caupolican complexes in the northwest, and the Ichilo
394 complex in the southeast; GEOBOL, 1979). Consequently, channel sinuosity is low
395 in general (<2 in most sub-reaches) and the upper end of this zone in particular has
396 experienced low migration rates ($< 5 \text{ ma}^{-1}$ in large areas). Further north, the western
397 side of the active channel belt is also bounded by clay bodies of the Ixiamas
398 complex, while in the east relatively few clay contacts were found. In this area, sub-
399 reaches 12 and 15 are strongly influenced by clay banks and exhibit a combination
400 of low migration rates ($< 20 \text{ ma}^{-1}$) and low sinuosity (< 2). In contrast, in sub-reaches
401 where meandering is relatively unconstrained (e.g., sub-reach 6, 9, 10, 14, 16)
402 migration rates are higher (27.0 ma^{-1} on average), cutoffs are frequent (Fig. 10) and
403 sinuosity is high (2.24 on average). Indeed, the transition between reaches in which
404 confining clay bodies are common and absent can be associated with a marked

change in channel planform character. For example, in sub-reach 6 downstream of bend 25 the channel leaves a zone where clay banks provide a strong stabilising influence. As a result, sinuosity increases and the channel belt widens, promoting rapid bend migration, increased cutoff frequency, rotation of bends, and the formation and cutoff of a multi-loop bend (Fig. 12). However, along the central section of the study reach, downstream propagation of this dynamic channel behaviour is prevented by the contact with the clay banks located further downstream (e.g. bend 35, Fig. 8).

413

414 **Numerical modelling**

The numerical model described above was applied to investigate the relationship between heterogeneity in bank erodibility and planform channel characteristics further. Model simulations were run for a period sufficient for the channel to develop a statistically steady form (i.e. without a long-term trend in channel sinuosity) and to rework the floodplain multiple times (8000 model iterations). Figure 13 shows the time series of channel sinuosity for model runs with contrasting k values. All simulations show a rapid initial increase in sinuosity as a meandering channel develops, as described by others (e.g., Howard and Knutson, 1984; Howard, 1992). Subsequently, sinuosity declines (following the first cutoff events) and then oscillates (reflecting the balance between channel lengthening, due to migration, and shortening, due to cutoffs). Figure 13 illustrates that spatial variability in erodibility (due to floodplain heterogeneity) promotes a substantial reduction in channel sinuosity. Moreover, simulation results are relatively insensitive to the precise value of k (for $k \geq 3$). For example, in the latter half of the simulation following the model

1
2
3
4
5
6
7
8
9
10
11
12
13
14
15
16
17
18
19
20
21
22
23
24
25
26
27
28
29
30
31
32
33
34
35
36
37
38
39
40
41
42
43
44
45
46
47
48
49
50
51
52
53
54
55
56
57
58
59
60

spin-up phase, mean sinuosity is 2.87 ($k = 0$), 2.05 ($k = 3$), and 2.07 ($k = 6$). Figure 14, shows that frequency distributions of channel curvature differ between simulations that neglect ($k = 0$) and account for floodplain heterogeneity ($k = 3$; note that the distribution for $k = 6$ is very similar). More specifically, spatial variability in heterogeneity promotes a curvature distribution similar to that observed on the Beni in sub-reaches where clay-rich banks are common, while neglecting spatial variability in erodibility leads to a distribution more similar to reaches along the Beni where clay banks are uncommon (Fig. 9).

Figure 15 shows the simulated planform pattern of floodplain sediment heterogeneity after 3900 iterations and the meandering channel position (at two instants in time) during model runs with constant bank erodibility ($k = 0$) and bank erodibility dependent on grain size assemblage ($k = 3$). It is evident from these plots that spatial variability in bank erodibility leads to a reduction in active channel belt width (by c. 35% on average), meander migration rates (by c. 40%) and cutoff frequency (by c. 50%), where the latter is indicated in Figure 15 by the number of abandoned channels that are characterised by a high proportion of fine sediment. Moreover, simulations in which bank erosion is dependent on floodplain grain size composition show several of the features of channel migration observed along the Rio Beni. These include the development of angular bend configurations, compounding, straightening downstream of contacts with fine sediment deposits and a tendency for the channel to become relatively immobile at locations where bank sediment is fine.

Discussion

1
2
3 453 The results presented above demonstrate that the spatial distribution of clay-rich
4
5 454 sediments within the floodplain of the Rio Beni exerts a significant influence on rates
6
7 455 of bank erosion, styles of meander migration, and channel morphology at bend and
8
9 456 channel-belt scales. The influence of floodplain heterogeneity on channel migration
10
11 457 has been recognised in many previous studies (e.g. Howard, 1996; Sun et al., 1996;
12
13 458 Huang and Nanson, 1998; Hudson and Kesel, 2000; Seminara, 2006, Gueneralp
14
15 459 and Rhoads, 2011; Motta et al., 2012a; Posner and Duan, 2012; Limaye and Lamb,
16
17 460 2014). However, the controls on and causes of heterogeneities in bank erodibility
18
19 461 remain to be understood fully. Several studies have focused on the influence on
20
21 462 channel migration of resistant clay plugs formed in oxbow lakes (e.g. Howard, 1996;
22
23 463 Sun et al., 1996; Hudson and Kesel, 2000). Similarly, it is in such locations that
24
25 464 resistance to erosion is highest in the simple numerical model utilised here. In
26
27 465 contrast, rates of bank erosion into channel cutoff sites are some of the most rapid
28
29 466 observed in this study (c. 140 ma^{-1} on average). This probably reflects the young age
30
31 467 of these cutoffs, which means that they have yet to be filled completely and the
32
33 468 sediment within them has not been consolidated or altered by pedogenic processes
34
35 469 (see also Gautier, 2007). The grain size of clay-rich banks is similar to that of
36
37 470 deposits found near the outlet of an oxbow lake (D_{50} : $1.5\text{--}3.0 \mu\text{m}$; Gautier et al.,
38
39 471 2010), which is a typical environment for the formation of clay plugs, although oxbow
40
41 472 lake deposits can be highly heterogeneous.

42
43
44
45
46
47
48 473 Overall, we find no consistent association between clay-rich bank material
49
50 474 and former channel locations along the Rio Beni, hence the origin of some of the
51
52 475 resistant bank sediments observed here remains uncertain. Moreover, previous
53
54 476 studies of channel migration along the Rio Beni that have investigated oxbow fill
55
56 477 processes provide no insight into the question of the evolution of resistant clay
57
58
59
60

1
2
3
4
5
6
7
8
9
10
11
12
13
14
15
16
17
18
19
20
21
22
23
24
25
26
27
28
29
30
31
32
33
34
35
36
37
38
39
40
41
42
43
44
45
46
47
48
49
50
51
52
53
54
55
56
57
58
59
60

bodies (e.g. Gautier et al., 2007; 2010). The clay-rich bank sediments observed along the Beni may have a range of origins, including fine-grained sedimentation within floodplain depressions, distal floodbasins, bar-top chute channels or remnants of mainstem cutoff infills (Fisk, 1947; Kolb, 1975; Schumm and Spitz, 1996). Image analysis confirms that clay bodies identified in bank sections have not been reworked since 1960, and that in many places the time since deposition of these sediments is likely to be much longer, although they may include a surface drape of more recent deposition. Clay-rich material with a similar mottled appearance (see Fig. 3a) was identified in floodplain sediments sampled in back swamp areas to the west of the Rio Beni and in older channel belts that are likely to have experienced slow sedimentation (perhaps $<1 \text{ mm a}^{-1}$, based on ^{210}Pb measurements from floodplain cores) over a prolonged time period (Aalto et al., 2003; Dumont, 1996). Based on these observations, we speculate that deposit age may be an important control on the properties and erodibility of these sediments, and that the resistant bank sediments observed here are likely hundreds to thousands of years old, and may thus be the product of prolonged sedimentation in distal floodbasins.

Our analysis suggests that the presence or absence of clay-rich bank sediment is the dominant spatial control on bank erosion rates along the Rio Beni. The resulting erosion rates are 60% and 48 % of those of coarser pointbar and channel deposits, while rates of bend migration into oxbow lakes are much greater and highly variable. The measured mean migration rates over many bends agree well with those of Gautier et al. (2007) for the same reach of the Beni although subdivision of bends into different sub-reaches prohibits direct comparison. Bank erosion rates were found to be unrelated to cutbank height or slope in the vicinity of the bend. Moreover, the relationship between mean bend curvature and migration

1
2
3 503 rate differs markedly between bends with and without clay-rich banks. For example,
4
5 504 at the former sites, migration rates are generally low over a wide range of curvatures
6
7 505 and thus largely independent of curvature. In the absence of clay rich banks,
8
9 506 migration rate is maximized at intermediate bend curvatures, as observed previously
10
11 507 for many freely meandering rivers (Nanson and Hickin, 1983; Hooke, 1997; Crosato,
12
13 508 2009). Temporally, mean annual bend migration rates are related to flood
14
15
16 509 magnitude, intensity and duration, as previously found by Gautier et al. (2007) on the
17
18 510 same river reach. However, we find that discharge metrics based on the previous
19
20 511 three wet seasons are better predictors of bank erosion rates than discharge metrics
21
22 512 based on a single wet season.
23
24
25

26 513 Channel morphology and styles of bend migration in the presence of clay-rich
27
28 514 deposits along the Rio Beni differ from the predictions of existing theory and simple
29
30 515 conceptual models, but are consistent with some past observations of channel
31
32 516 behaviour. For example, where the apex and the downstream limb of a bend is in
33
34 517 contact with a clay-rich bank, faster down-valley translation of the more mobile
35
36 518 upstream limb leads to a reduction in wave length, up-valley skewing (e.g. bend 24
37
38 519 in Fig. 12), and eventually to neck cutoff. Similar processes have been described
39
40 520 previously for the Mississippi River (Fisk, 1947). The observed decrease in channel
41
42 521 width downstream of the bend apex, where the channel is immobilised by resistant
43
44 522 banks, contrasts with the peak in width at this location that has been associated with
45
46 523 'free-meandering bends' (Luchi et al., 2011; Zolezzi et al., 2012). However, this
47
48 524 difference in channel morphology is consistent with the difference in boundary
49
50 525 conditions, and serves to emphasize the significant control exerted by variable bank
51
52 526 strength. Overall, fewer than 10% of bends are characterised by styles of
53
54 527 development that fit simple conceptual models of bend evolution (Hickin, 1978;
55
56
57
58
59
60

1
2
3
4
5
6
7
8
9
10
11
12
13
14
15
16
17
18
19
20
21
22
23
24
25
26
27
28
29
30
31
32
33
34
35
36
37
38
39
40
41
42
43
44
45
46
47
48
49
50
51
52
53
54
55
56
57
58
59
60

Hooke, 1987) and associated changes in migration rate between inception and cutoff (Hooke and Yorke, 2010). This can be attributed, in part, to the influence of heterogeneity in floodplain composition on bend migration and planform shape. For example, during a period of straightening in sub-reach 7 downstream of the clay contact in bend 35 a number of cutoffs occurred (Fig. 8) but instead of a gradual increase in sinuosity, as predicted by conceptual models (Hooke, 2003), the reach continued to straighten until 2005. Such cutoff avalanches are typical for meandering rivers and have been observed along the Beni (Gautier et al., 2007) and elsewhere (Stolum, 1996; Hooke, 2004), but the concurrent medium-term straightening is less common.

In general, there appears to be an inverse relationship between clay body frequency and mean annual migration rate and channel sinuosity, which is related to the role of clay banks in reducing bank erosion and promoting channel straightening. However, this tendency over-simplifies the relationship between clay body frequency and channel dynamics. For example, sub-reach 8 is characterised by very low sinuosity and migration rates despite a lack of contact with clay-rich bank sections. More generally, although migration rates at clay banks tend to be low, average rates within sub-reaches where clay-banks are common need not necessarily be low if migration rates between these immobile locations are enhanced. Figure 16 shows that in sub-reaches 1 to 8 the apices of bends where clay-rich banks have been found in 2011 have not moved significantly over up to five decades, and that channel migration occurs only between these bends. Thus, bends with resistant clay-rich banks can act as fixed hinges around which the channel migrates. Even where cutoffs occur immediately upstream of these fixed points this has relatively little impact on the position of these bends, and usually results in only short-term and

1
2
3 553 limited bend translation (e.g., for 3 years at bend 18, Fig. 12a). Since planform
4
5 554 adjustment downstream of cutoffs is suppressed, new bends formed at the cutoff
6
7 555 tend to lengthen and extend rapidly (e.g., bends 16 and 20 in Figs. 6c and 12c).
8
9 556 When bends with clay-rich banks are cut off, this can result in a short-term increase
10
11 557 in migration rate and can lead to a change in migration direction into substrate of
12
13 558 different erodibility, thereby further increasing mobility (e.g., downstream of bend 43
14
15 559 after 2003, see Fig. 8e, f). Consequently, floodplain heterogeneity may also modify
16
17 560 the characteristic dynamics of channel evolution by promoting long periods of
18
19 561 stability punctuated by rapid channel adjustment when the influence of clay-rich
20
21 562 banks is temporarily removed. Moreover, the straight channels found downstream of
22
23 563 clay-rich bends may decouple these bends from planform evolution downstream if
24
25 564 the spacing between clay-rich bends is sufficient (e.g. between bend 20 and 24, but
26
27 565 not below bend 24 (Fig. 12d)).
28
29
30
31

32
33 566 Channel behaviour in sub-reaches 11 and 17 to 19 deviates from the
34
35 567 relationships identified above. For example, there are few clay bodies exposed along
36
37 568 channel bank lines in these areas, they are relatively stable (migration rates $< 20 \text{ m a}^{-1}$
38
39 569 ¹), and yet are characterised by relatively high sinuosity (Fig. 11). Sub-reaches 17 to
40
41 570 19 lie towards the downstream end of the Beni foredeep, hence channel evolution in
42
43 571 this area is likely controlled in part by tectonics. For example, downstream of the
44
45 572 study reach the channel is bounded by higher terraces that are indicative of vertical
46
47 573 displacement of the channel bed relative to the surrounding floodplain. Gautier et al.
48
49 574 (2007) emphasize the role of tectonics in promoting low slopes and channel incision,
50
51 575 which in turn leads to lateral channel stability downstream of the junction between
52
53 576 the Rio Beni and the Rio Madidi. It is possible that these effects extend further
54
55 577 upstream beyond the junction with the Madidi into the study site considered here.
56
57
58
59
60

1
2
3
4
5
6
7
8
9
10
11
12
13
14
15
16
17
18
19
20
21
22
23
24
25
26
27
28
29
30
31
32
33
34
35
36
37
38
39
40
41
42
43
44
45
46
47
48
49
50
51
52
53
54
55
56
57
58
59
60

578 However, the limited dGPS data that we obtained in this area indicate a steepening
579 of the channel water surface upstream of the Madidi. Moreover, channel stability in
580 sub-reaches 17 to 19 over the past few decades is not necessarily representative of
581 longer-term channel evolution, and the floodplain in this area contains ample
582 evidence of previous channel migration, abandonment and bifurcation.

583 The model results presented here illustrate that the simulation model captures
584 many of the effects of spatial variability in bank erodibility, despite the simplicity of
585 the process parameterisations used. Moreover, they support the conclusion that
586 floodplain heterogeneity may have a substantial influence on channel geometry and
587 styles of bend evolution. These results are consistent with those of previous
588 modelling studies that have highlighted the effects of heterogeneity in bank strength
589 on channel belt width (Sun et al., 1996) and meander dynamics (Gueneralp and
590 Rhoads, 2011). However, the current simulations also suggest that heterogeneity in
591 floodplain alluvium can promote a substantial reduction in channel sinuosity, which
592 would in turn have significant implications for channel gradient, flow conveyance,
593 sediment transport and, potentially, basin accommodation space. The differences in
594 channel behaviour simulated by these models likely reflects several factors, including
595 differences in the underlying meander migration models used, their parameterisation
596 of bank erodibility, and their ability to simulate spatial structure in floodplain
597 heterogeneity. As a consequence of this, the true sensitivity of channel behaviour to
598 heterogeneity in bank composition is difficult to quantify accurately using these
599 models, due to their phenomenological nature. Resolving this issue likely requires
600 the use of models with a stronger physical basis. Specifically, such models should:
601 (i) incorporate a physically-based (and perhaps fully three-dimensional) treatment of
602 hydrodynamics that is suitable for representing the controls on boundary shear

stress in channels with complex planform geometries; (ii) be capable of representing streamwise variations in channel width and depth linked to pinning of bend apices by resistant floodplain sediments; (iii) include an improved treatment of floodplain sediment conveyance and sedimentation, and the physical and chemical processes that control the long-term evolution of floodplain sediment properties and erodibility. Development of such a model represents a significant challenge because the nature of and controls on long-term post-depositional changes in floodplain sediment properties are poorly understood. Moreover, requirements (i) and (iii) are, to some extent, mutually exclusive in that they may require the application of computationally expensive hydrodynamic models over periods of millennia.

613

614 **Conclusions**

Many previous studies have hypothesized that spatial heterogeneity in floodplain sediments and associated bank erodibility may represent an important control on the evolution of alluvial meanders. This study has quantified these effects for the case of the Rio Beni, Bolivia, which is a large dynamic sand-bed river, characterised by high average rates of channel migration and overbank sedimentation. Field data and GIS analysis demonstrate that floodplain clay bodies along the Rio Beni are a key control on meander form and evolution at spatial scales ranging from individual bends up to distances of several tens of kilometers. While the origin of these clay deposits is not certain, we find no simple association between recent cutoff channels and the location of clay bodies. Rather, we speculate that clay rich bodies may be a product of slow sedimentation in distal flood basins, and that pedogenic processes may be an important control on the long-term evolution of floodplain erodibility.

1
2
3
4
5
6
7
8
9
10
11
12
13
14
15
16
17
18
19
20
21
22
23
24
25
26
27
28
29
30
31
32
33
34
35
36
37
38
39
40
41
42
43
44
45
46
47
48
49
50
51
52
53
54
55
56
57
58
59
60

627 Bends that interact with such clay bodies are associated with a significant
628 reduction in migration rate and channel width, and a change in the frequency
629 distribution of local channel curvature that is linked to the formation of more angular
630 geometries characterised by sharp bends and extended straight channel segments.
631 At larger spatial scales, clay bodies act as hinge points that can limit the upstream
632 and downstream propagation of morphodynamic perturbations (e.g., bend translation
633 and response to cutoff). As a consequence, the spatial distribution of clay bodies can
634 promote marked streamwise changes in meander sinuosity and dynamics (over
635 distances of 10-50 km).

636 Our numerical model results are consistent with field observations, and imply
637 that spatial heterogeneity in bank erodibility driven by variable bank composition may
638 drive a substantial (c. 30%) reduction in average channel sinuosity, compared to
639 situations in which bank strength is spatially homogeneous. Moreover, this effect is
640 not simply a consequence of a reduction in average bank erodibility. Rather, reduced
641 channel migration rates and sinuosity are driven, in part, by the change in the
642 curvature distribution of the channel. Thus, the increase in the length of straight
643 channel segments and the creation of sharp bends near clay bodies may both
644 influence the streamwise development of secondary flows and reduce rates of bank
645 erosion. Although the simple modelling framework employed does not represent flow
646 hydrodynamics or sediment transport processes, it does appear to provide a first
647 order representation of the link between floodplain erodibility and meander geometry
648 that supports this conclusion.

649 These results illustrate that heterogeneity in floodplain sedimentology is a first
650 order control on channel planform and dynamics. Moreover, by controlling channel
651 belt width, lateral channel migration and levee reworking, floodplain heterogeneity is

likely an important influence on the geometry and rate of aggradation of alluvial ridges, the frequency of avulsions and the resulting basin alluvial architecture. Since the spatial-scaling of floodplain heterogeneity is linked to the processes (and associated scales) that control floodplain construction, these effects cannot be accounted for fully in numerical models using stochastically-generated patterns of floodplain erodibility. Rather, attempts to model and thus understand meander dynamics, even over relatively short time scales (e.g., 10-100 years), may need to simulate time periods that are long enough to represent the evolution of floodplain heterogeneity and the bi-directional feedbacks with channel morphodynamics.

661

662 **Acknowledgements**

663 This research was funded by the UK Natural Environment Research Council (grant
664 NE/H009108/1). We are grateful to the two referees, whose comments led to
665 improvements in the manuscript.

666

1
2
3
4
5
6
7
8
9
10
11
12
13
14
15
16
17
18
19
20
21
22
23
24
25
26
27
28
29
30
31
32
33
34
35
36
37
38
39
40
41
42
43
44
45
46
47
48
49
50
51
52
53
54
55
56
57
58
59
60

References

Aalto R, Maurice-Bourgoin L, Dunne T, Montgomery DR, Nitttrouer CA, Guyot JL.
2003. Episodic sediment accumulation on Amazonian flood plains influenced
by El Nino/Southern Oscillation. *Nature* **425**: 493-497.

Allenby RJ. 1988. Origin of rectangular and aligned lakes in the Beni Basin of
Bolivia. *Tectonophysics* **145**: 1-20.

Brice JC. 1974. Evolution of meander loops. *Geological Society of America Bulletin*
85: 581-586.

Camporeale C, Perona P, Porporato A, Ridolfi L. 2005. On the long-term behavior of
meandering rivers. *Water Resources Research* **41**: W12403.

Camporeale C, Ridolfi L. 2006. Convective nature of the planimetric instability in
meandering river dynamics. *Physical Review E* **73**: 026311.

Constantine CR, Dunne T, Hanson GJ. 2009. Examining the physical meaning of the
bank erosion coefficient used in meander migration modeling.
Geomorphology **106**: 242-252.

Crosato A. 2009. Physical explanations in river meander migration rates from model
comparison. *Earth Surface Processes and Landforms* **34**: 2078-2086.

Dumont JF. 1996. Neotectonics of the Subandes-Brazilian craton boundary using
geomorphological data: The Marañon and Beni basins. *Tectonophysics* **259**:
137-151.

Dumont JF, Hannagarth W. 1993. River shifting and tectonics in the Beni basin.
Third International Conference Geomorphology, Hamilton.

Ferguson RI. 1984. Kinematic model of meander migration. In *River meandering*,
Elliot CM (ed.). ASCE: New York; 942-951.

- 691 Fisk HN. 1947. Fine-grained alluvial deposits and their effects on Mississippi River
692 activity. *USCE Mississippi River Communications* **1**: 82.
- 693 Frascati A, Lanzoni S. 2010. Long-term river meandering as a part of chaotic
694 dynamics? A contribution from mathematical modelling. *Earth Surface
695 Processes and Landforms* **35**: 791-802.
- 696 Gautier E, Brunstein D, Vauchel P, Jouanneau J-M, Roulet M, Garcia C, Guyot JL,
697 Castro M. 2010. Channel and floodplain sediment dynamics in a reach of the
698 tropical meandering Rio Beni (Bolivian Amazonia). *Earth Surface Processes
699 and Landforms* **35**: 1838-1853.
- 700 Gautier E, Brunstein D, Vauchel P, Roulet M, Fuertes O, Guyot JL, Darozzes J,
701 Bourrel L. 2007. Temporal relations between meander deformation, water
702 discharge and sediment fluxes in the floodplain of the Rio Beni (Bolivian
703 Amazonia). *Earth Surface Processes and Landforms* **32**: 230-248.
- 704 GEOBOL. 1979. Complejos de Tierra del Oriente Boliviano. In *ERTS*, Brockmann
705 CE (ed.). Servicio Geologico de Bolivia: La Paz.
- 706 Gueneralp I, Abad JD, Zolezzi G, Hooke J. 2012. Advances and challenges in
707 meandering channels research. *Geomorphology* **163-164**: 1-9.
- 708 Gueneralp I, Marston RA. 2012. Process-form linkages in meander
709 morphodynamics: Bridging theoretical modeling and real world complexity.
710 *Progress in Physical Geography* **36**: 718-746.
- 711 Gueneralp I, Rhoads BL. 2011. Influence of floodplain erosional heterogeneity on
712 planform complexity of meandering rivers. *Geophysical Research Letters* **38**:
713 L14401.

- 1
2
3 714 Guyot JL, Jouanneau JM, Wasson JG. 1999. Characterisation of river bed and
4
5 715 suspended sediments in the Rio Madeira drainage basin (Bolivian Amazonia).
6
7 716 *Journal of South American Earth Sciences* **12**: 401-410.
8
9
10 717 Guyot JL, Jouanneau JM, Soares L, Boaventura GR, Maillet N, Lagane C. 2007.
11
12 718 Clay mineral composition of river sediments in the Amazon Basin. *Catena* **71**:
13
14 719 340-356.
15
16 720 Hickin E. 1978. Mean flow structure in meanders of the Squamish River, British
17
18 721 Columbia. *Canadian Journal of Earth Sciences* **15**: 1833-1849.
19
20
21 722 Hickin EJ. 1974. The development of meanders in natural river-channels. *American*
22
23 723 *Journal of Science* **274**: 414-442.
24
25 724 Hooke J.M. 1984. Change in river meanders: a review of techniques and results of
26
27 725 analyses. *Progress in Physical Geography* **8**: 473-508.
28
29 726 Hooke JM. 1987. Changes in meander morphology. In *International Geomorphology*
30
31 727 *1986*, Gardiner V (ed.). Wiley: Chichester; 591-609.
32
33
34 728 Hooke JM. 1995. River channel adjustment to meander cutoffs on the River Bollin
35
36 729 and River Dane, northwest England. *Geomorphology* **14**: 235-253.
37
38 730 Hooke JM. 1997. Styles of channel change. In *River engineering and management*,
39
40 731 Thorne CR, Hey RD, Newson MD (eds.). John Wiley & Sons: Chichester;
41
42 732 237-268.
43
44
45 733 Hooke JM. 2003. River meander behaviour and instability: a framework for analysis.
46
47 734 *Transactions of the Institute of British Geographers* **28**: 238-253.
48
49 735 Hooke JM. 2004. Cutoffs galore!: occurrence and causes of multiple cutoffs on a
50
51 736 meandering river. *Geomorphology* **61**: 225-238.
52
53
54
55
56
57
58
59
60

- 1
2
3 737 Hooke JM, Yorke L. 2010. Rates, distributions and mechanisms of change in
4
5 738 meander morphology over decadal timescales, River Dane, UK. *Earth*
6
7 739 *Surface Processes and Landforms* **35**: 1601-1614.
8
9
10 740 Howard AD. 1992. Modeling channel migration and floodplain sedimentation in
11
12 741 meandering streams. In *Lowland floodplain rivers: geomorphological*
13
14 742 *perspectives*, Carling PA, Petts GE (eds.). John Wiley & Sons: Chichester; 1-
15
16 743 41.
17
18 744 Howard AD. 1996. Modelling channel evolution and floodplain morphology. In
19
20 745 *Floodplain Processes*, Anderson MG, Walling DE, Bates PD (eds.). John
21
22 746 Wiley & Sons: Chichester; 15-62.
23
24 747 Howard AD, Knutson TR. 1984. Sufficient conditions for river meandering: a
25
26 748 simulation approach. *Water Resources Research* **20**: 1659-1667.
27
28
29 749 Huang HQ, Nanson GC. 1998. The influence of bank strength on channel geometry:
30
31 750 An integrated analysis of some observations. *Earth Surface Processes and*
32
33 751 *Landforms* **23**: 865-876.
34
35
36 752 Hudson PF, Kesel RH. 2000. Channel migration and meander-bend curvature in the
37
38 753 lower Mississippi River prior to major human modification. *Geology* **28**: 531-
39
40 754 534.
41
42
43 755 Ikeda S, Parker G, Sawai K. 1981. Bend theory of river meanders .1. Linear
44
45 756 development. *Journal of Fluid Mechanics* **112**: 363-377.
46
47 757 Johannesson H, Parker G. 1989. Linear theory of river meanders. In *River*
48
49 758 *meandering*, Ikeda S, Parker G (eds.). AGU: Washington; 181-214.
50
51
52 759 Julian JP, Torres R. 2006. Hydraulic erosion of cohesive river banks.
53
54 760 *Geomorphology* **76**: 193-206.
55
56
57
58
59
60

- 1
2
3 761 Kolb CR. 1975. Geologic control of sand boils along Mississippi River levees. US
4
5 762 Army Engineer Waterways Experiment Station: Vicksburg.
6
7 763 Lancaster ST, Bras RL. 2002. A simple model of river meandering and its
8
9 764 comparison to natural channels. *Hydrological Processes* **16**: 1-26.
10
11 765 Latrubesse EM, Restrepo JD. 2014. Sediment yield along the Andes: continental
12
13 766 budget, regional variations, and comparisons with other basins from orogenic
14
15 767 mountain belts. *Geomorphology* **216**: 225-233.
16
17 768 Lauer JW, Parker G. 2008. Modeling framework for sediment deposition, storage,
18
19 769 and evacuation in the floodplain of a meandering river: Theory. *Water*
20
21 770 *Resources Research* **44**: W04425.
22
23 771 Limaye ABS, Lamb MP. 2014. Numerical simulations of bedrock valley evolution by
24
25 772 meandering rivers with variable bank material, *Journal of Geophysical*
26
27 773 *Research – Earth Surface* doi: 10.1002/2013JF002997
28
29 774 Luchi R, Zolezzi G, Tubino M. 2011. Bend theory of river meanders with spatial width
30
31 775 variations. *Journal of Fluid Mechanics* **681**: 311-339.
32
33 776 Mackey SD, Bridge JS. 1995. Three-dimensional model of alluvial stratigraphy:
34
35 777 Theory and application, *Journal of Sedimentary Research* **B65**: 7-31.
36
37 778 Motta D, Abad JD, Langendoen EJ, Garcia MH. 2012a. The effects of floodplain soil
38
39 779 heterogeneity on meander planform shape. *Water Resources Research* **48**:
40
41 780 W09518.
42
43 781 Motta D, Abad JD, Langendoen EJ, Garcia MH. 2012b. A simplified 2D model for
44
45 782 meander migration with physically-based bank evolution. *Geomorphology*
46
47 783 **163-164**: 10-25.
48
49 784 Nanson GC, Hickin EJ. 1983. Channel Migration and Incision on the Beatton River.
50
51 785 *Journal of Hydraulic Engineering* **109**: 327-337.
52
53
54
55
56
57
58
59
60

- 1
2
3 786 Nanson GC, Hickin EJ. 1986. A statistical analysis of bank erosion and channel
4
5 787 migration in western Canada. *Geological Society of America Bulletin* **97**: 497-
6
7 788 504.
8
9
10 789 Parker G, Shimizu Y, Wilkerson GV, Eke EC, Abad JD, Lauer JW, Paola C, Dietrich
11
12 790 WE, Voller VR. 2011. A new framework for modeling the migration of
13
14 791 meandering rivers. *Earth Surface Processes and Landforms* **36**: 70-86.
15
16 792 Perucca E, Camporeale C, Ridolfi L. 2007. Significance of the riparian vegetation
17
18 793 dynamics on meandering river morphodynamics. *Water Resources Research*
19
20 **43**: W03430.
21
22
23 795 Plafker G. 1964. Oriented lakes and lineaments of Northeastern Bolivia. *Geological*
24
25 796 *Society of America Bulletin* **75**: 503-522.
26
27 797 Posner AJ, Duan JG. 2012. Simulating river meandering processes using stochastic
28
29 798 bank erosion coefficient. *Geomorphology* **163-164**: 26-36.
30
31
32 799 Salo J, Kalliola R, Häkkinen I, Mäkinen Y, Niemelä P, Puhakka M, Coley PD. 1986.
33
34 800 River dynamics and the diversity of Amazon lowland forest. *Nature* **322**: 254-
35
36 801 258.
37
38 802 Schumm SA, Spitz WJ. 1996. Geological influences on the Lower Mississippi River
39
40 803 and its alluvial valley. *Engineering Geology* **45**: 245-261.
41
42
43 804 Seminara G. 2006. Meanders. *Journal of Fluid Mechanics* **554**: 271-297.
44
45 805 Stolum H-H. 1996. River meandering as a self-organization process. *Science* **271**:
46
47 806 1710-1713.
48
49 807 Sun T, Meakin P, Jossang T, Schwarz K. 1996. A simulation model for meandering
50
51 808 rivers. *Water Resources Research* **32**: 2937-2954.
52
53
54
55
56
57
58
59
60

1
2
3
4
5
6
7
8
9
10
11
12
13
14
15
16
17
18
19
20
21
22
23
24
25
26
27
28
29
30
31
32
33
34
35
36
37
38
39
40
41
42
43
44
45
46
47
48
49
50
51
52
53
54
55
56
57
58
59
60

809 van de Wiel MJ, Darby SE. 2007. A new model to analyse the impact of woody
810 riparian vegetation on the geotechnical stability of riverbanks. *Earth Surface*
811 *Processes and Landforms* **32**: 2185-2198.

812 Ward JV, Tockner K, Arscott DB, Claret C. 2002. Riverine landscape diversity.
813 *Freshwater Biology* **47**: 517-539.

814 Xu D, Bai Y, Ma J, Tan Y. 2011. Numerical investigation of long-term planform
815 dynamics and stability of river meandering on fluvial floodplains.
816 *Geomorphology* **132**: 195-207.

817 Zolezzi G, Luchi R, Tubino M. 2012. Modeling morphodynamic processes in
818 meandering rivers with spatial width variations. *Reviews of Geophysics* **50**:
819 RG4005.

820 Zolezzi G, Seminara G. 2001. Downstream and upstream influence in river
821 meandering. Part 1. General theory and application to overdeepening. *Journal*
822 *of Fluid Mechanics* **438**: 183-211.

823

824

Table 1: Aerial and satellite imagery used for GIS analysis of migration patterns. All Landsat scenes are from Path 001, Row 069 and 070. Rectification errors (relative to the year 2000 Landsat images or SRTM in 2000) are given for both tiles or combined tiles where applicable.

Date	Type of image	Resolution (pixel size)	Rectification RMSE
1960	aerial		>30 m
October 1975	Landsat LM2	83 m	>30 m
August 1987	Landsat LT5	30 m	>30 m
August 1993	Landsat LT5	30 m	>30 m
July 1996	Landsat LT5	30 m	76.7 m
August 1997	Landsat LT5	30 m	11.9 - 14.7 m
July 1998	Landsat LT5	30 m	18.0
July/ August 1999	Landsat LE7	30 m	7.5 - 11.7 m
July/ August 2000	Landsat LE7	30 m	8.8 - 9.3 m (relative to SRTM)
June/ August 2001	Landsat LE7	30 m	9.2 - 18.4 m
August 2003	Landsat LT5	30 m	8.2 - 15.6 m
September 2004	Landsat LT5	30 m	8.2 - 15.6 m
September 2005	Landsat LT5	30 m	8.2 - 15.6 m
July 2006	Landsat LT5	30 m	8.2 - 15.6 m
August 2007	Landsat LT5	30 m	8.2 - 15.6 m
August 2008	Landsat LT5	30 m	8.2 - 15.6 m
August 2009	Landsat LT5	30 m	8.2 - 15.6 m
May 2010	Landsat LT5	30 m	6.8 - 7.3 m
May/ June 2011	Landsat LT5	30 m	8.2 - 15.6 m

1
2
3
4
5
6
7
8
9
10
11
12
13
14
15
16
17
18
19
20
21
22
23
24
25
26
27
28
29
30
31
32
33
34
35
36
37
38
39
40
41
42
43
44
45
46
47
48
49
50
51
52
53
54
55
56
57
58
59
60

Figure Captions

Figure 1: a) Location of the Rio Beni, northeastern Bolivia; b) Rio Beni study reach showing sub-reach boundaries and areas used to illustrate channel dynamics in figures 6, 8 and 12. The background Landsat TM imagery was taken during the dry season 2011.

Figure 2: Dominant styles of meander bend migration along the study reach: a) Compounding; b) Expansion; c) Extension; d) Lateral displacement; e) Rotation; and f) Longitudinal translation. Adapted from Hooke (1984). The red outline shows the bank lines some time before the Landsat image was taken.

Figure 3: Typical bank sections along the study reach: a) Stable cutbank consisting of clay-rich material at Bend 72; b) Bank composed of silty, highly erodible sediments, with evidence of vertical layering.

Figure 4: Mean migration rates of bends of the Rio Beni between 1960 and 2011 (95 % confidence intervals shown as error bars). Bends are classified by the substrate or the morphological feature into which they are migrating: banks composed of mixed-sized sediments, clay-rich banks, silty and sandy point bar (and counter point bar) deposits, active oxbow lakes, and former channels infilled with mixed-sized sediments.

Figure 5: Proportion of bends within the 19 sub-reaches experiencing different styles of migration between 1960 and 2011. Sub-reaches 1, 3-5, 7, 12 and 15 are dominated by clay-rich banks.

Figure 6: Typical sequence of channel migration influenced by clay-rich banks between bends 13 and 18 (in sub-reach 4) over the periods: a) 1975-1987; b) 1987-

1993; and c) 1993-1996. Landsat image dates correspond to the end of each time period while banklines shown in red represent the start of the time period in each panel. The presence of resistant clay-rich cutbanks in bend 13, 14 and 18 (marked orange in c) limit rates of bend migration and lead to up-valley skewing of mature bends, such as bend 14. Flow direction is indicated by the arrow.

Figure 7: Changes over time in the length of straight channel segments (identified in the key by the sub-reach number in which they are located), illustrating the gradual down-valley lengthening that occurs over multiple decades downstream of clay-rich banks. Typically these segments lengthen due to down-valley translation, increase in bend wavelength and cutoff of bends downstream (solid lines), but contact with other clay-rich banks can lead to the development of perturbations and thus termination of the lengthening process (dashed lines). This process is also illustrated in Fig. 8e and 8f. Each line represents a single channel segment.

Figure 8: Migration of the Rio Beni between bends 34 and 44 over the periods: a) 1987-1993; b) 1993-1998; c) 1998-2001; d) 2001-2005; e) 2005-2011, and f) 2011-2013. Landsat image dates correspond to the end of each time period while banklines shown in red represent the start of the time period in each panel. The channel in this location (sub-reach 7) straightens between 1998 and 2005, following a series of cutoffs. Flow direction is indicated by an arrow and relevant bend numbers are given. Exposed clay-rich banks were found at bend 35 and 40 (marked orange in e and f).

Figure 9: Frequency distribution of channel curvature at sub-reaches that are dominated by clay-rich banks (sub-reaches 1, 3-5, 7, 12 and 15) compared with the remaining sub-reaches with few clay-rich banks.

Figure 10: Mean centerline migration rates for the 19 sub-reaches along the Rio Beni over four periods between 1960 and 2011. Symbols indicate the proportion of the channel in each sub-reach experiencing mean migration rates above and below threshold values (5 ma^{-1} and 50 ma^{-1} , respectively). Arrows at the top of the image indicate the occurrence of chute (grey) and neck (black) cutoffs.

Figure 11: Mean channel sinuosity for the 19 sub-reaches along the Rio Beni at five points in time between 1960 and 2011.

Figure 12: Migration of the Rio Beni between bends 18 and 29 over the periods: a) 1993-1996; b) 1996-2001; c) 2001-2003; d) 2003-2009; and e) 2009-2011. Landsat image dates correspond to the end of each time period while banklines shown in red represent the start of the time period in each panel. Flow direction is indicated by an arrow and relevant bend numbers are given. Exposed clay-rich banks (marked orange in e) were found at bend 18, 20, 22, 24, 25, 26 and 29.

Figure 13: Time series of channel sinuosity for three numerical model simulations in which the dependence of bank erodibility on grain size composition is altered by changing the value of k in equation (2).

Figure 14: Frequency distributions of channel curvature for simulations in which bank erodibility is constant ($k = 0$) and bank erodibility varies as a function of grain size composition ($k = 3$).

Figure 15: Spatial patterns of the fraction of fine sediment in the floodplain and the meandering channel position (at two instants in time) during model simulations in which bank erodibility is constant (upper panel; $k = 0$) and bank erodibility varies as a function of grain size composition (lower panel; $k = 3$).

Figure 16: Channel centre lines between 1960 and 2011 in the upper study reach (sub-reaches 1-8) with arrows marking bends with clay-rich banks (orange lines). These bends are relatively immobile over >50 years and act as fixed 'hinges' between more mobile reaches (see text). Flow is from left to right (in order A-B-C).

For Peer Review

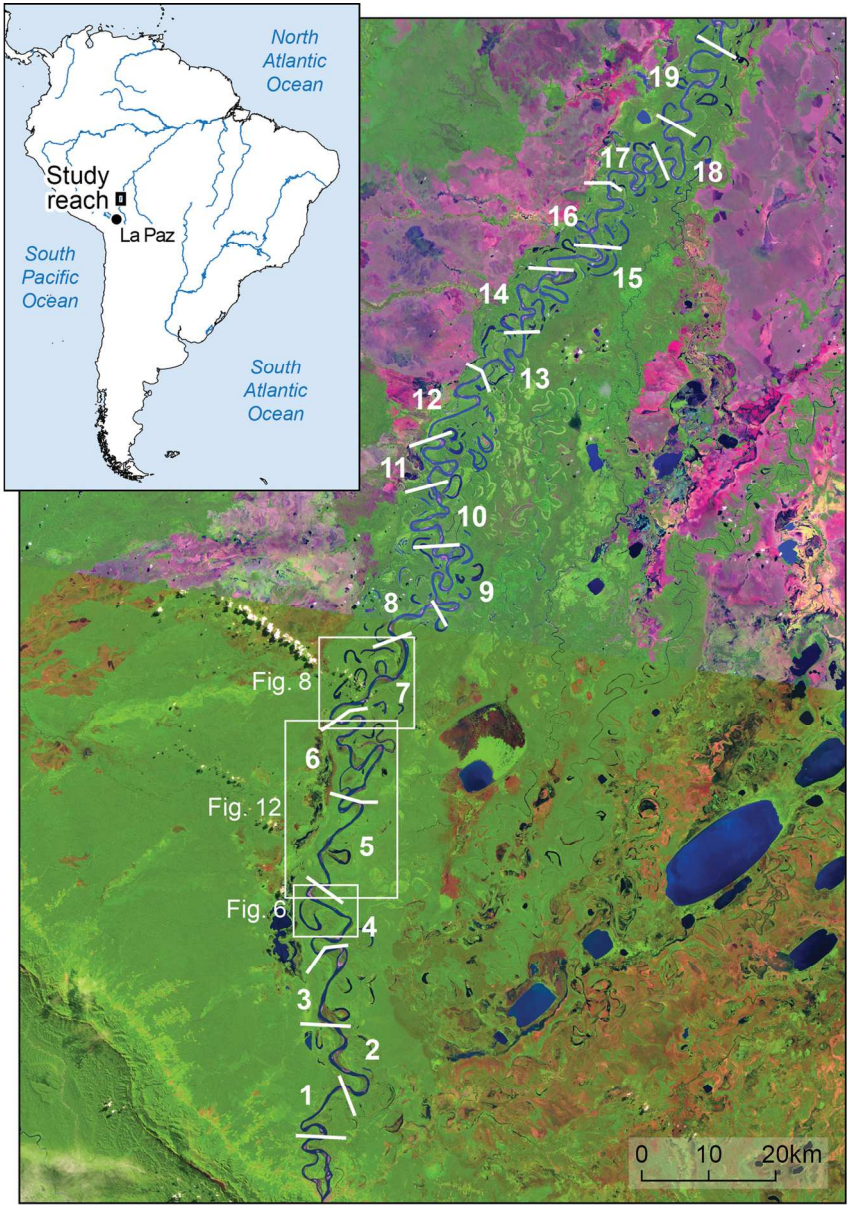


Figure 1: a) Location of the Rio Beni, northeastern Bolivia; b) Rio Beni study reach showing sub-reach boundaries and areas used to illustrate channel dynamics in figures 6, 8 and 12. The background Landsat TM imagery was taken during the dry season 2011.
119x170mm (300 x 300 DPI)

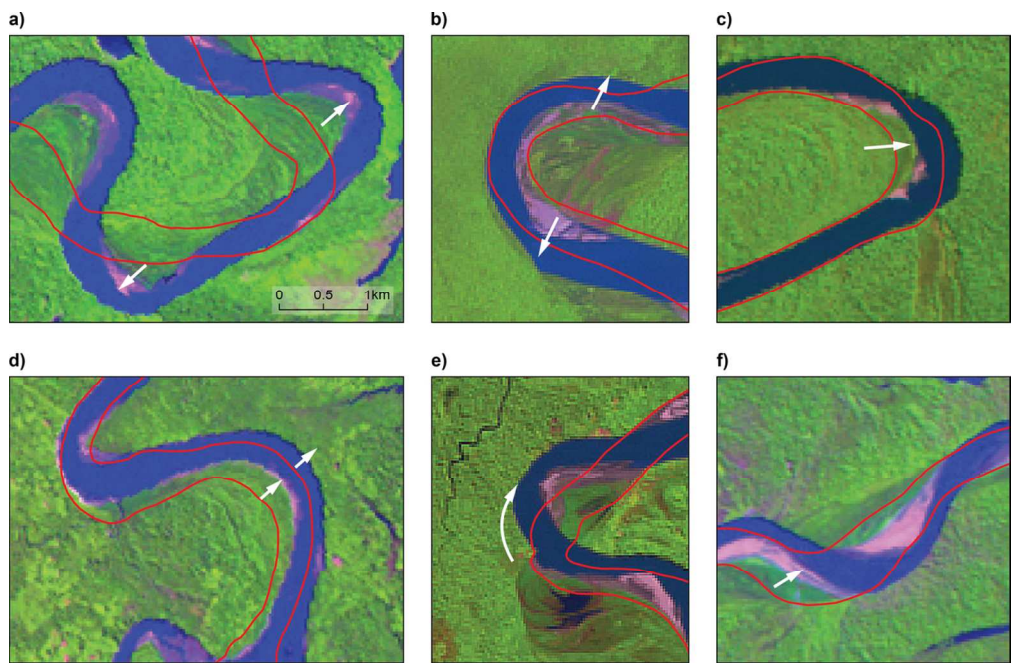


Figure 2: Dominant styles of meander bend migration along the study reach: a) Compounding; b) Expansion; c) Extension; d) Lateral displacement; e) Rotation; and f) Longitudinal translation. Adapted from Hooke (1984). The red outline shows the bank lines some time before the Landsat image was taken.
114x74mm (300 x 300 DPI)

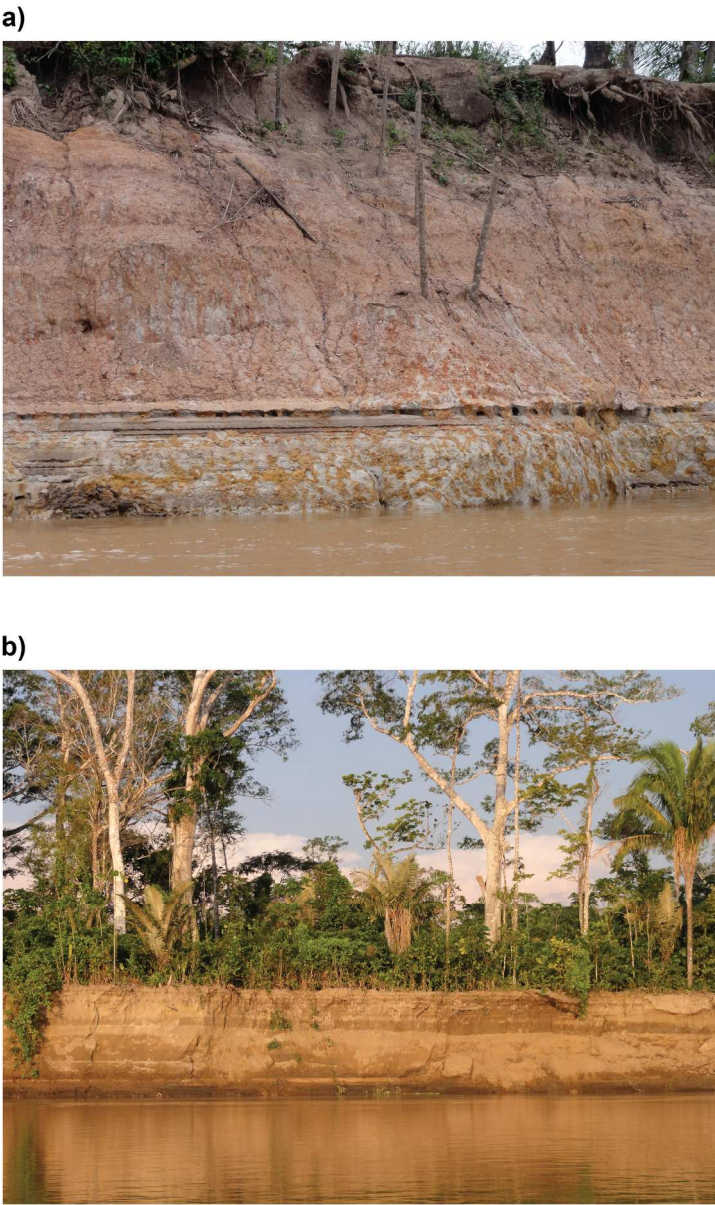


Figure 3: Typical bank sections along the study reach: a) Stable cutbank consisting of clay-rich material at Bend 72; b) Bank composed of silty, highly erodible sediments, with evidence of vertical layering.
141x237mm (300 x 300 DPI)

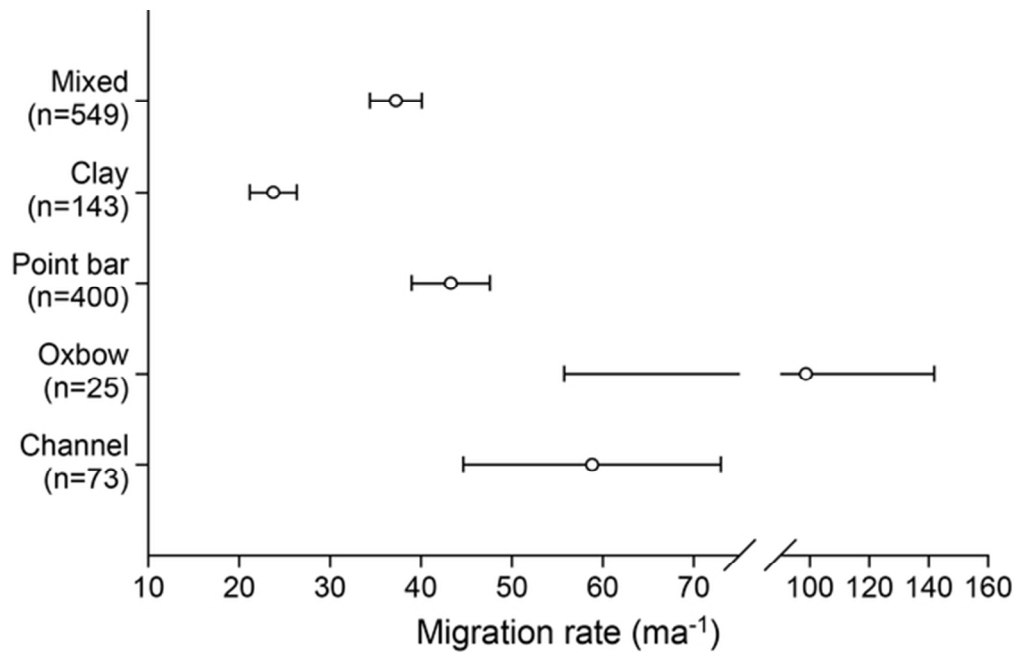


Figure 4: Mean migration rates of bends of the Rio Beni between 1960 and 2011 (95 % confidence intervals shown as error bars). Bends are classified by the substrate or the morphological feature into which they are migrating: banks composed of mixed-sized sediments, clay-rich banks, silty and sandy point bar (and counter point bar) deposits, active oxbow lakes, and former channels infilled with mixed sediments.
54x34mm (300 x 300 DPI)

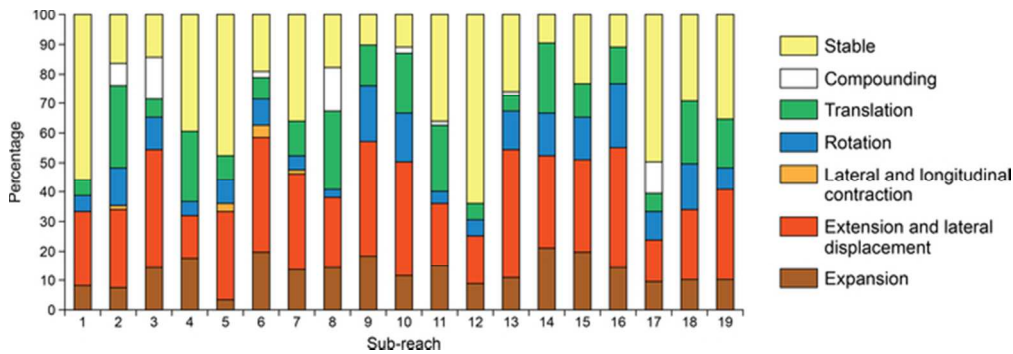


Figure 5: Proportion of bends within the 19 sub-reaches experiencing different styles of migration between 1960 and 2011. Sub-reaches 1, 3-5, 7, 12 and 15 are dominated by clay-rich banks.
59x20mm (300 x 300 DPI)

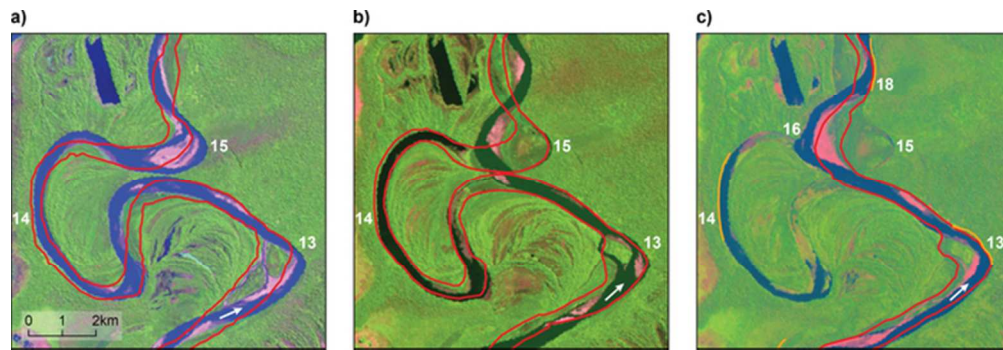


Figure 6: Typical sequence of channel migration influenced by clay-rich banks between bends 13 and 18 (in sub-reach 4) over the periods: a) 1975-1987; b) 1987-1993; and c) 1993-1996. Landsat image dates correspond to the end of each time period while banklines shown in red represent the start of the time period in each panel. The presence of resistant clay-rich cutbanks in bend 13, 14 and 18 (marked orange in c) limit rates of bend migration and lead to up-valley skewing of mature bends, such as bend 14. Flow direction is indicated by the arrow.
59x19mm (300 x 300 DPI)

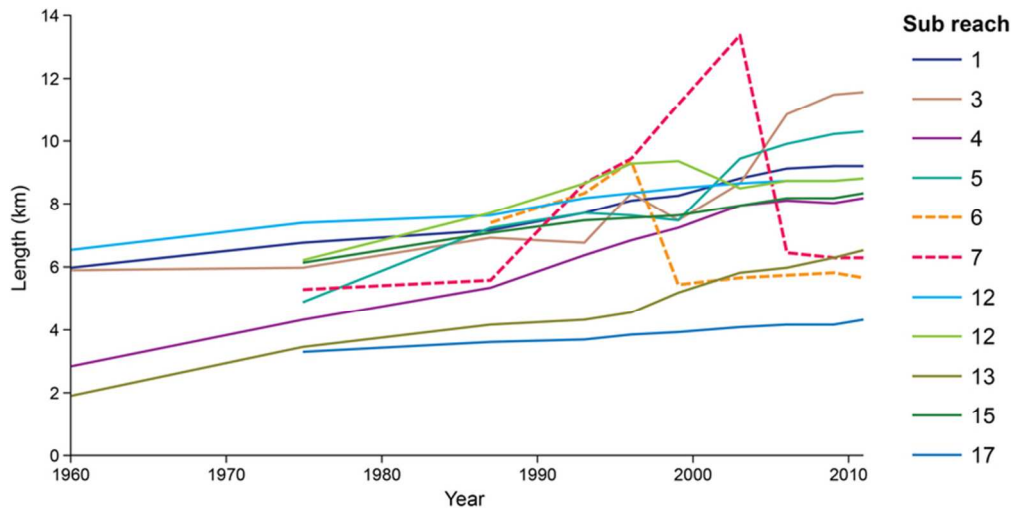


Figure 7: Changes over time in the length of straight channel segments (identified in the key by the sub-reach number in which they are located), illustrating the gradual down-valley lengthening that occurs over multiple decades downstream of clay-rich banks. Typically these segments lengthen due to down-valley translation, increase in bend wavelength and cutoff of bends downstream (solid lines), but contact with other clay-rich banks can lead to the development of perturbations and thus termination of the lengthening process (dashed lines). This process is also illustrated in Fig. 8e and 8f. Each line represents a single channel segment.

72x36mm (300 x 300 DPI)

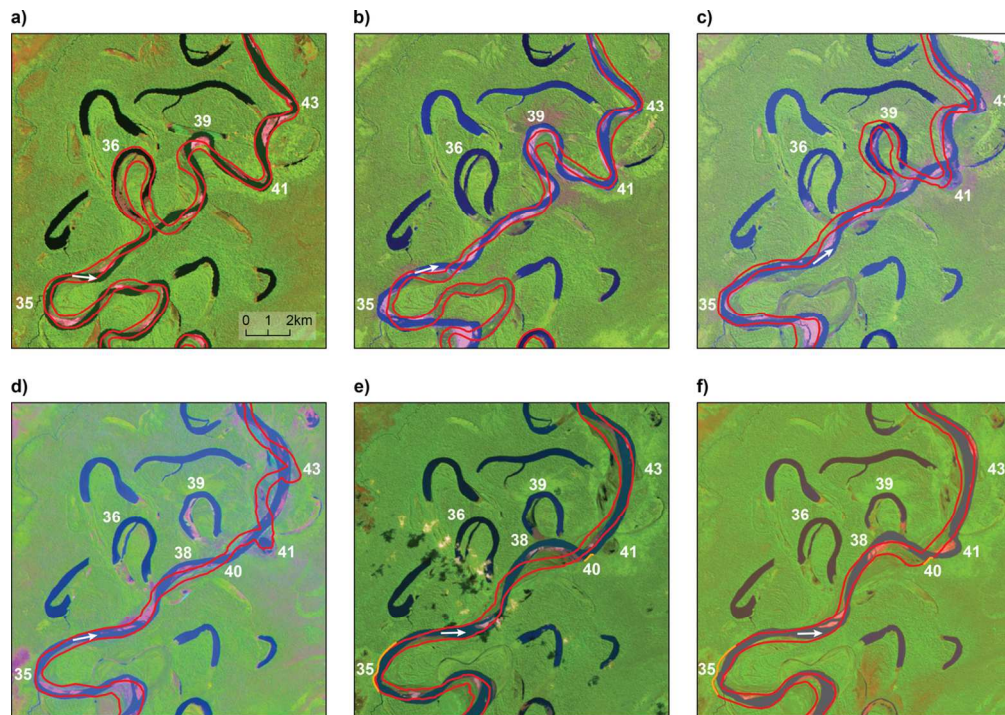


Figure 8: Migration of the Rio Beni between bends 34 and 44 over the periods: a) 1987-1993; b) 1993-1998; c) 1998-2001; d) 2001-2005; e) 2005-2011, and f) 2011-2013. Landsat image dates correspond to the end of each time period while banklines shown in red represent the start of the time period in each panel. The channel in this location (sub-reach 7) straightens between 1998 and 2005, following a series of cutoffs. Flow direction is indicated by an arrow and relevant bend numbers are given. Exposed clay-rich banks were found at bend 35 and 40 (marked orange in e and f).

123x87mm (300 x 300 DPI)

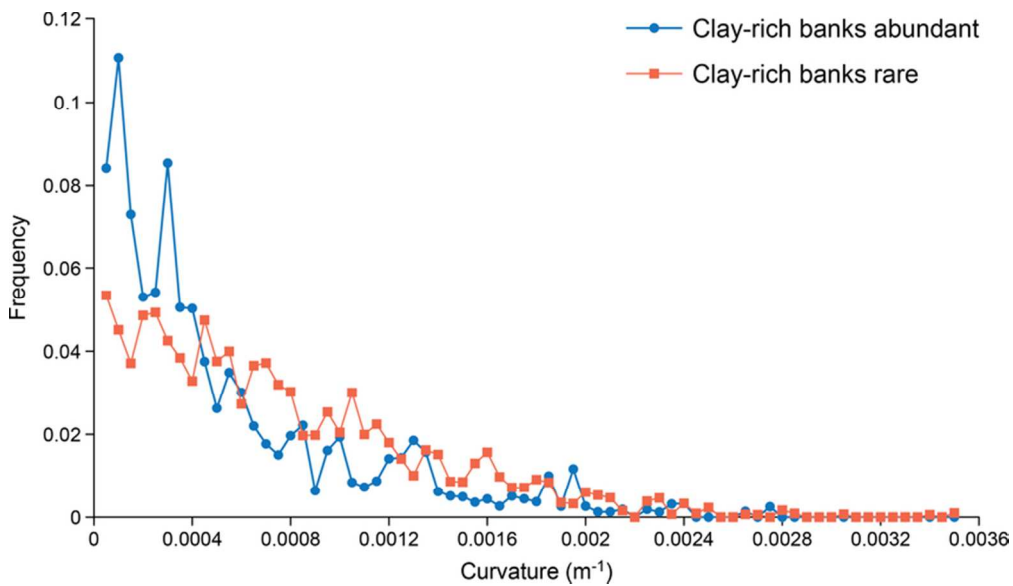


Figure 9: Frequency distribution of channel curvature at sub-reaches that are dominated by clay-rich banks (sub-reaches 1, 3-5, 7, 12 and 15) compared with the remaining sub-reaches with few clay-rich banks. 71x41mm (300 x 300 DPI)

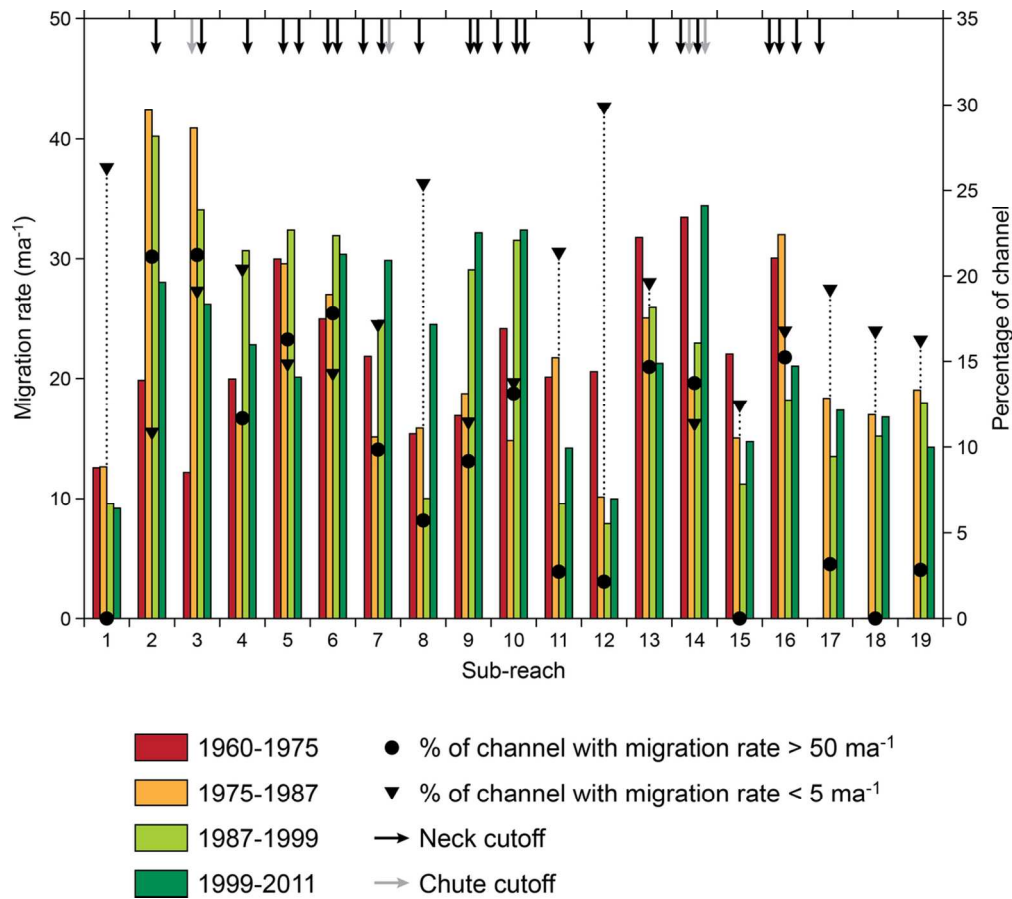


Figure 10: Mean centerline migration rates for the 19 sub-reaches along the Rio Beni over four periods between 1960 and 2011. Symbols indicate the proportion of the channel in each sub-reach experiencing mean migration rates above and below threshold values (5 ma⁻¹ and 50 ma⁻¹, respectively). Arrows at the top of the image indicate the occurrence of chute (grey) and neck (black) cutoffs.

110x98mm (300 x 300 DPI)

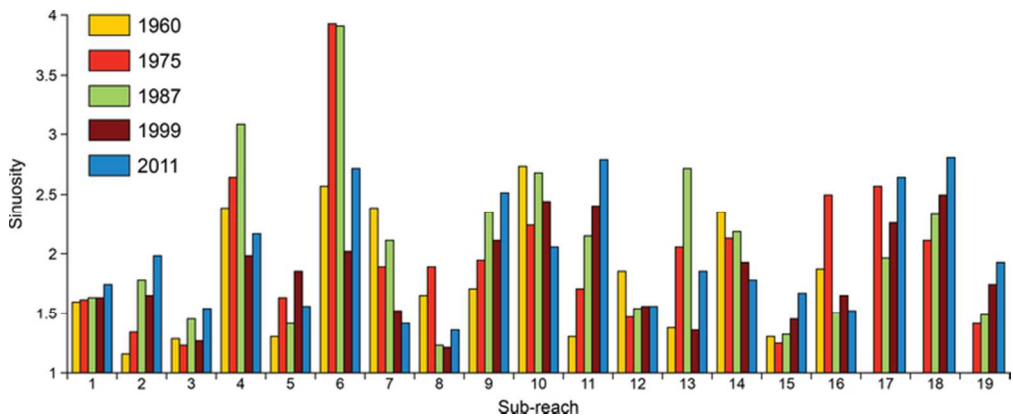


Figure 11: Mean channel sinuosity for the 19 sub-reaches along the Rio Beni at five points in time between 1960 and 2011.
65x26mm (300 x 300 DPI)

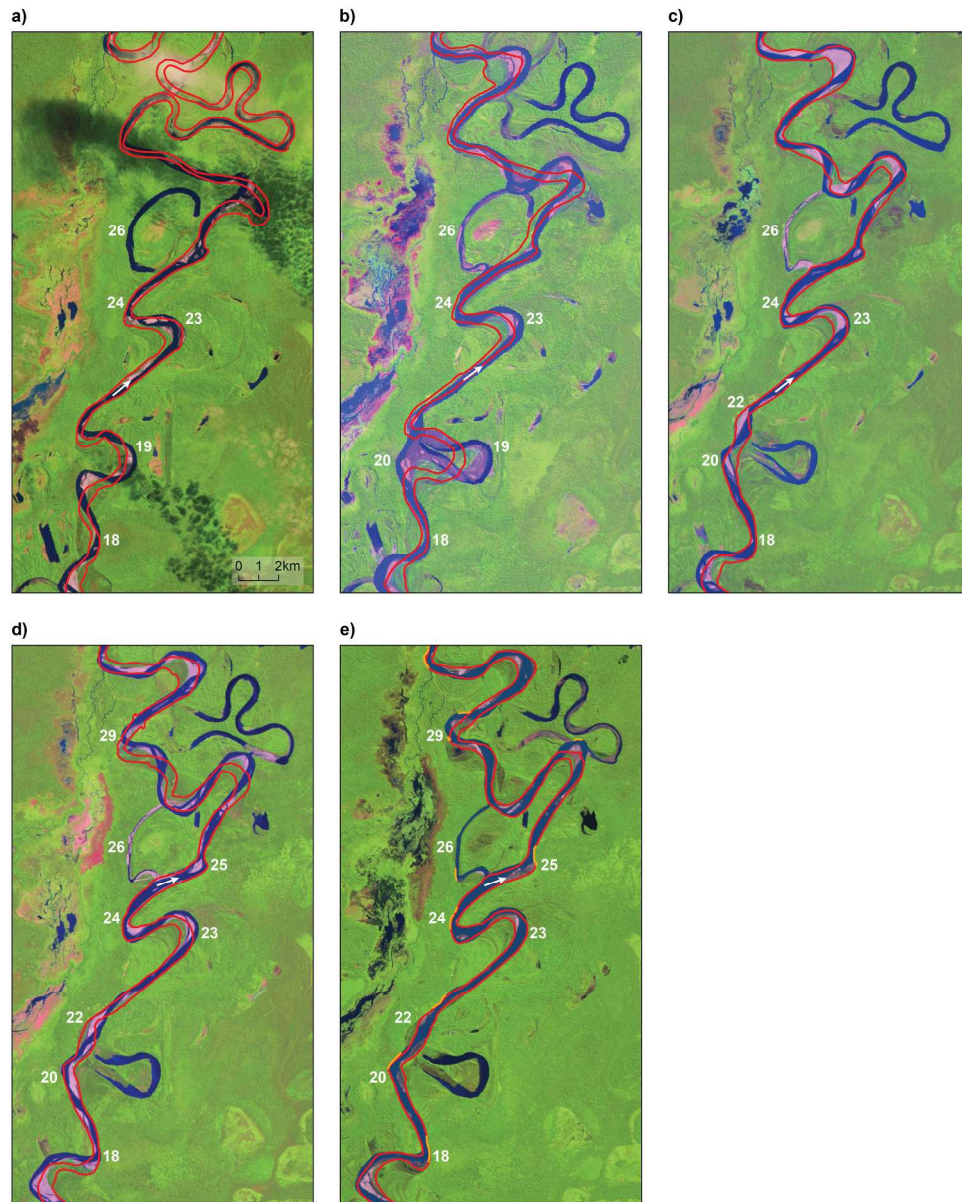


Figure 12: Migration of the Rio Beni between bends 18 and 29 over the periods: a) 1993-1996; b) 1996-2001; c) 2001-2003; d) 2003-2009; and e) 2009-2011. Landsat image dates correspond to the end of each time period while banklines shown in red represent the start of the time period in each panel. Flow direction is indicated by an arrow and relevant bend numbers are given. Exposed clay-rich banks (marked orange in e) were found at bend 18, 20, 22, 24, 25, 26 and 29.

218x272mm (300 x 300 DPI)

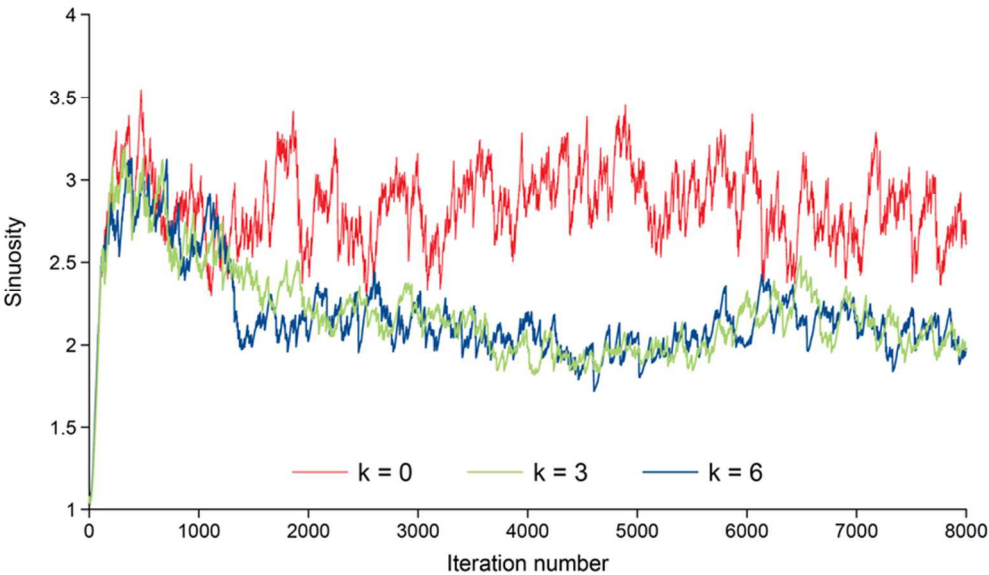


Figure 13: Time series of channel sinuosity for three numerical model simulations in which the dependence of bank erodibility on grain size composition is altered by changing the value of k in equation (2).
73x42mm (300 x 300 DPI)

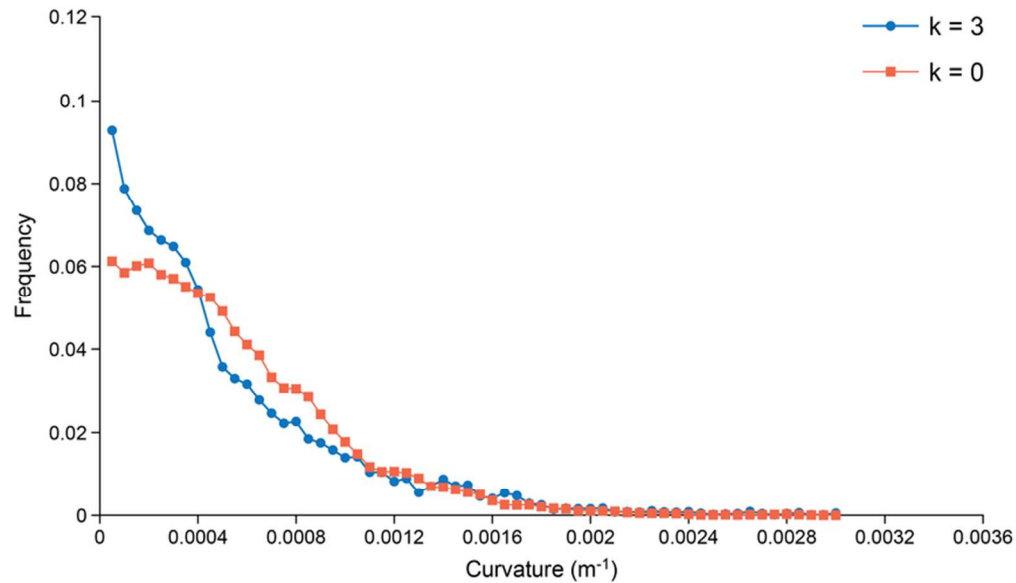


Figure 14: Frequency distributions of channel curvature for simulations in which bank erodibility is constant ($k = 0$) and bank erodibility varies as a function of grain size composition ($k = 3$).
72x41mm (300 x 300 DPI)

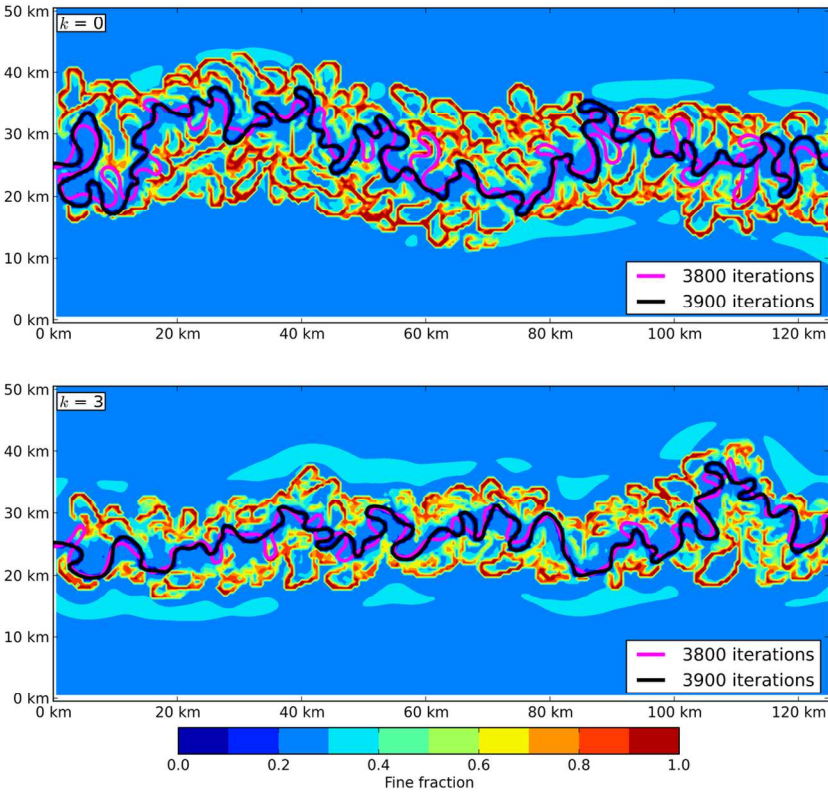


Figure 15: Spatial patterns of the fraction of fine sediment in the floodplain and the meandering channel position (at two instants in time) during model simulations in which bank erodibility is constant (upper panel; $k = 0$) and bank erodibility varies as a function of grain size composition (lower panel; $k = 3$).
127x110mm (300 x 300 DPI)

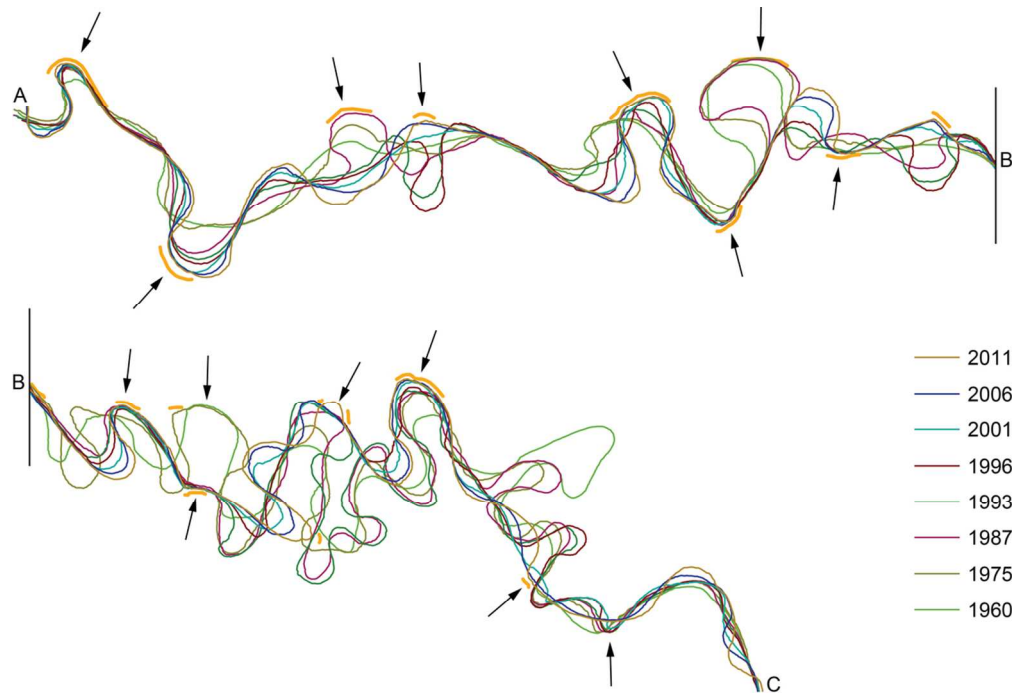


Figure 16: Channel centre lines between 1960 and 2011 in the upper study reach (sub-reaches 1-8) with arrows marking bends with clay-rich banks (orange lines). These bends are relatively immobile over >50 years and act as fixed 'hinges' between more mobile reaches (see text). Flow is from left to right (in order A-B-C).

107x74mm (300 x 300 DPI)